Performance Testing of Crumb Rubber Modified Hot Mix Asphaltic Concrete

Research Report 0-4821-2
Project Number 0-4821

Conducted for

Texas Department of Transportation
P.O. Box 5080
Austin, Texas 78763

March 2006

Center for Transportation Infrastructure Systems
The University of Texas at El Paso
El Paso, Texas 79968
(915) 747-6925

1. Report No. FHWA/TX-06/0-4821-2	2. Government Accession No.	3. Recipient's Catalog No.	
4. Title and Subtitle Performance Testing of Crumb Rubber Modified Hot Mix Asphaltic Concrete		5. Report Date March 2006	
		6. Performing Organization Code	
7. Author(s) Vaibhav Swami, M.S. Vivek Tandon, PhD, PE Soheil Nazarian, PhD, PE Aleksander Zborowski, B.S. Kamil E. Kaloush, PhD, PE		8. Performing Organization Report No. 0-4821-2	
9. Performing Organization Name and Address Center for Transportation Infrastructure Systems The University of Texas at El Paso El Paso, Texas 79968-0516		10. Work Unit No.	
		11. Contract or Grant No. 0-4821	
12. Sponsoring Agency Name and Address Texas Department of Transportation Research and Technology Implementation Office P.O. Box 5080 Austin, Texas 78763		13. Type of Report and Period Covered Technical Report: September 04 thru December 05	
		14. Sponsoring Agency Code	
15. Supplementary Notes Research performed in cooperation with the Texas Department of Transportation and the Federal Highway Administration. *Project title:* Mix Design and Performance Testing of Crumb Rubber Modified Hot Mix Asphaltic Concrete (CRM-HMAC)			

16. Abstract

Crumb-rubber is typically used to improve the durability of hot-mix asphalt concrete. Although hot-mix asphalt concrete containing crumb-rubber has been successfully placed and has performed well over the years, the performance evaluation of these mixes has been an elusive task. Hamburg Wheel Tracking Device Test or static creep tests, typically specified by TxDOT, have not been able to consistently predict the performance of these mixes. Various performance tests were selected and evaluated using four mixes containing crumb-rubber to recommend a suitable performance test for these materials. The experiment design and evaluation tests results are presented in this report.

17. Key Words CRM-HMAC, HWTD, Flow time, Flow number, Dynamic modulus, Static creep, and Flexural fatigue.	18. Distribution Statement No restrictions. This document is available to the public through the National Technical Information Service, Spring field, Virginia 22161, www.ntis.gov		
19. Security Classif. (of this report) Unclassified	20. Security Classif. (of this page) Unclassified	21. No. of Pages 87	22. Price

Performance Testing of Crumb Rubber Modified Hot Mix Asphaltic Concrete

By

Vaibhav Swami, M.S.
Vivek Tandon, PhD, PE
Soheil Nazarian, PhD, PE
Aleksander Zborowski, B.S.
Kamil E. Kaloush, PhD, PE

Report Number 0-4821-2
Project Number 0-4821

Project Title: Mix Design and Performance Testing of Crumb Rubber Modified Hot Mix Asphaltic Concrete (CRM-HMAC)

Performed in cooperation with the

Texas Department of Transportation and the Federal Highway Administration

Disclaimer:

The contents of this report reflect the view of the authors, who are responsible for the facts and the accuracy of the data presented herein. The contents do not necessarily reflect the official views or policies of the Texas Department of Transportation or the Federal Highway Administration. This report does not constitute a standard, specification, or regulation.

NOT INTENDED FOR CONSTRUCTION, BIDDING, OR PERMIT PURPOSES

Vaibhav Swami, MS
Vivek Tandon, PhD, PE (88219)
Soheil Nazarian, PhD, PE (69263)
Aleksander Zborowski, BS
Kamil E. Kaloush, PhD, PE

ACKNOWLEDGEMENTS

ABSTRACT

Crumb-rubber is typically used to improve the durability of hot-mix asphalt concrete. Although hot-mix asphalt concrete containing crumb-rubber has been successfully placed and has performed well over the years, the performance evaluation of these mixes has been an elusive task. Hamburg Wheel Tracking Device Test or static creep tests, typically specified by TxDOT, have not been able to consistently predict the performance of these mixes. Various performance tests were selected and evaluated using four mixes containing crumb-rubber to recommend a suitable performance test for these materials. The experiment design and evaluation tests results are presented in this report.

TABLE OF CONTENTS

LIST OF FIGURES

LIST OF TABLES

CHAPTER 1   INTRODUCTION

1.1   PROBLEM STATEMENT

Crumb-rubber (CRM) is typically added to improve the durability (resistance to cracking and rutting) of hot mix asphalt concrete (HMAC). The modified mix is commonly known as CRM-HMAC. The CRM is typically added and mixed to the asphalt cement before mixing it with the aggregates through a process commonly known as the wet process. Another advantage of the CRM is that it reduces the temperature susceptibility of the HMAC as shown in Figure 1. The use of the CRM also allows for the safe disposal of a large number of waste tires with minimal environmental concerns.
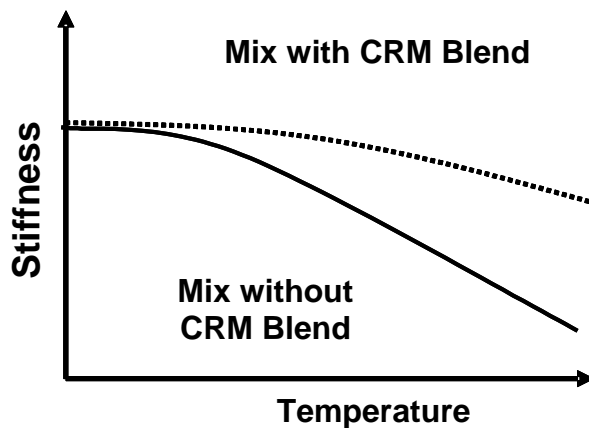
FIGURE 1   Influence of Temperature on Stiffness of HMAC Consisting of CRM Blend

Although the CRM-HMAC pavements have been successfully placed and have performed well over the years, the laboratory preparation of specimens in some cases has proven to be problematic. The sources of the problem include the stickiness of crumb-rubber asphalt cement, the temperature and method of mixing crumb rubber in asphalt cement, the expansion of specimens after removal from the mold, etc. Another issue specific to TxDOT is the current mix design procedure (Tex-232-F). This procedure is perceived to be cumbersome since quite a large number of laboratory specimens are required before the appropriate mix design of the CRM-HMAC can be determined. Occasionally, the mix design using laboratory-prepared mixes differs from the mix design using plant-produced mixes.

The CRM-HMAC mixes that perform well in the field often fail the Hamburg Wheel Tracking Device (HWTD) tests as specified in Tex-242-F. Another commonly specified test to evaluate the performance of the CRM-HMAC mixes is the static creep test (Tex-231-F). The static creep test has questionable repeatability. In addition, the specimens for the test method Tex-232-F are prepared with the Texas Gyratory compactor (TGC). However, the new mixture performance tests, including the HWTD, are carried out on specimens prepared with the Superpave Gyratory Compactor (SGC).

In view of the above discussion, the CRM-HMAC mix design procedure (Tex-232-F) needs to be modified to reduce the specimen preparation time, to streamline the specimen preparation and handling process, to ensure that mix design based on plant mixes or laboratory-prepared specimens are similar, and to include the SGC device in the specimen preparation. In addition, a suitable performance test setup needs to be identified that is repeatable and can be easily performed in the laboratory.

As part of this study, Swami et al. (2005) proposed a streamlined procedure to include steps for molding CRM-HMAC specimens using the TGC or SGC. The evaluation of several alternative performance test methods is included in this report.

1.2   OBJECTIVE

The main objective of this study is to identify and evaluate existing laboratory performance test methods that are repeatable and can be easily performed. To achieve this objective, three different plant mixes of known field performance were selected and evaluated. In addition, one mix was produced in the laboratory using modified Tex-232-F procedure. A literature review was also performed to identify existing and emerging performance tests that can be utilized to consistently identify performance of CRM-HMAC.

1.3   ORGANIZATION OF THE REPORT

Problem statement, research objective and organization of the report are presented in this chapter. In Chapter Two, the background information and research approach is presented. The results of the evaluation of various performance tests are included in Chapter Three. The summary and conclusion are included in Chapter Four.

CHAPTER 2   PERFORMANCE TESTS FOR CRM-HMAC MIXES

Performance testing of CRM-HMAC mixes has been problematic. Currently, TxDOT specifies the HWTD test (Tex-242-F) or static creep test (Tex-231-F). However, the HWTD test has typically yielded poor results on mixes that are similar in design and material components to those that have historically performed well under traffic. Although static creep tests have provided results that are more representative of field performance, the repeatability of that test procedure has been of concern.

With the current trend towards mechanistic pavement design and the need for more reliable design procedure, accurate characterization of the CRM-HMAC properties is vital. Witczak et al. (2002) under the National Cooperative Highway Research Program (NCHRP) Project 9-19, proposed several new tests commonly known as "Simple Performance Tests (SPT)." These tests include dynamic modulus to predict the permanent deformation and fatigue cracking, axial repeated (flow number) test to predict the permanent deformation, and axial creep (flow time) test to predict the permanent deformation. The dynamic modulus test is also recommended in the new mechanistic design guide. In addition, Nazarian et al. (2003) have demonstrated that the dynamic modulus tests and seismic tests can be combined to obtain a master curve to be used as a field acceptance criterion.

Kaloush et al. (2002) have evaluated the CRM-HMAC mixtures using SPT tests and have indicated that the flow number and flow time tests could be used to identify the benefits of the CRM. Kaloush studied two mix types that contain CRM: gap-graded mixtures and open-graded mixtures. Typical results of tests performed on those mixes suggested that change in shear resistance is identified by SPT tests.

The Strategic Highway Research Program (SHRP) has advocated an indirect tensile (IDT) strength test to measure the creep-compliance and strength of HMAC (AASHTO TP9-94). The test is performed to assess the low-temperature cracking potential of HMAC. Kaloush (2002) conducted these tests on a number of CRM-HMAC specimens, and concluded that the CRM-HMAC mixes with higher strain at failure have higher resistance to thermal cracking.

An AASHTO test method for determining the fatigue life of compacted HMAC is the flexural beam fatigue test (AASHTO TP8-94). The test is performed to estimate the fatigue life of the HMAC beam specimens. The specimen is subjected to repeated flexural bending loads until failure. A stiffness reduction of more than 50% (after 10,000 cycles) corresponds to failure. Typically, these test needs to be performed at a minimum of four strain levels and three temperatures. A minimum of 60 hours of testing is required to complete fatigue tests. In addition, the specimen preparation process is cumbersome and requires more than 10 hours to prepare each specimen. Kaloush et al. (2002) and Sousa et al. (2002) have indicated that the fatigue life is greater for CRM mixes as compared to the conventional mixes. Although fatigue tests can be used to quantify the benefits of the CRM in the HMAC mixes, it is difficult to perform them on regular basis because of the time constraints.

Based on the literature review, the HWTD, static creep, dynamic modulus, flow number, flow time, and indirect tensile tests have potential of identifying performance of CRM-HMAC. Therefore, these tests were evaluated to identify a suitable test than can reliably predict performance of CRM-HMAC in the laboratory. In addition, flexural fatigue beam and seismic tests were performed to document the properties of the CRM in the HMAC. The background information on each test procedure and expected performance measurements are reported in the following sections.

2.1   Hamburg Wheel Tracking Device (Tex-242-F)

The Hamburg Wheel Tracking Device has been used in Germany as a specification tool since the mid 1970's. Since Hamburg is the major seaport for Germany, the roads are subjected to a large number of heavily loaded, slow moving trucks. The Road Authority uses the Wheel Tracking Device Test as a specification requirement for their most severely stressed pavements. This device has been adopted by several SHAs including TxDOT.

The Hamburg Wheel Tracking Device (Figure 2) measures the combined effects of rutting and moisture damage by rolling a steel wheel across the surface of an asphalt concrete test specimen that is immersed in hot water. Each steel wheel makes up to 20,000 passes or until 20 mm of deformation is reached. The results that are customarily reported include the depth of deformation versus the number of wheel passes. The test setup is designed for testing slab specimens. However, with the increasing use of the gyratory compactor, TxDOT has adopted a test protocol that uses cylindrical specimens compacted in the SGC (Izzo and Tahmoressi, 1999).

FIGURE 2   Hamburg Wheel Tracking Device Test Set Up

The only disadvantage of this test is that it does not provide a fundamental property that can be used for modeling purposes. Recommended values for specific climates and traffic levels are also not available (Solaimanian et al., 2004). However, the test is easy to perform and is part of the TxDOT acceptance criterion (ITEM 346).

2.1.1 Test Procedure and Calculations for HWTD Tests

To perform tests, four specimens are compacted to a density of $93 \pm 1\%$ using a SGC. The compacted specimens, which are 6 in. (150 ± 2 mm) in diameter and 2.5 in. (62 ± 2 mm) in height, are cooled to room temperature for a period of 24 hr. The four specimens are then divided into two groups. Edge of each specimen is then trimmed with a masonry saw. The trimming is approximately 5/8 in. (16 mm). The specimens are placed in an acrylic mold and then placed in a mounting tray. The thickness of the acrylic mold is 2.4 in. (60 mm). The specimens in the mold are labeled with the percent air voids, mix type and height.

Information regarding the specimens and water temperature are entered into the computer. The mounting trays are then fastened to the empty water bath. The water bath is filled with water and heated to 122^oF (50^oC). The test specimens are allowed to saturate in the water bath for an additional 60 minutes once the 122^oF (50^oC) water temperature is reached. This waiting time is also referred to as start delay time. Once the test starts, the specimens are maintained in the heated water bath for 307 minutes. The test is automatically stopped when the required number of passes or when the maximum allowable rutting depth of 0.5 in. (12.5 mm) is reached. The number of passes to failure or the final rut depth is recorded at the end of the test. A typical test result is shown in Figure 3 indicating that the mix meets the TxDOT criterion of less than 0.5 in. (12.5 mm) deformation at the end of the 20,000 cycles.
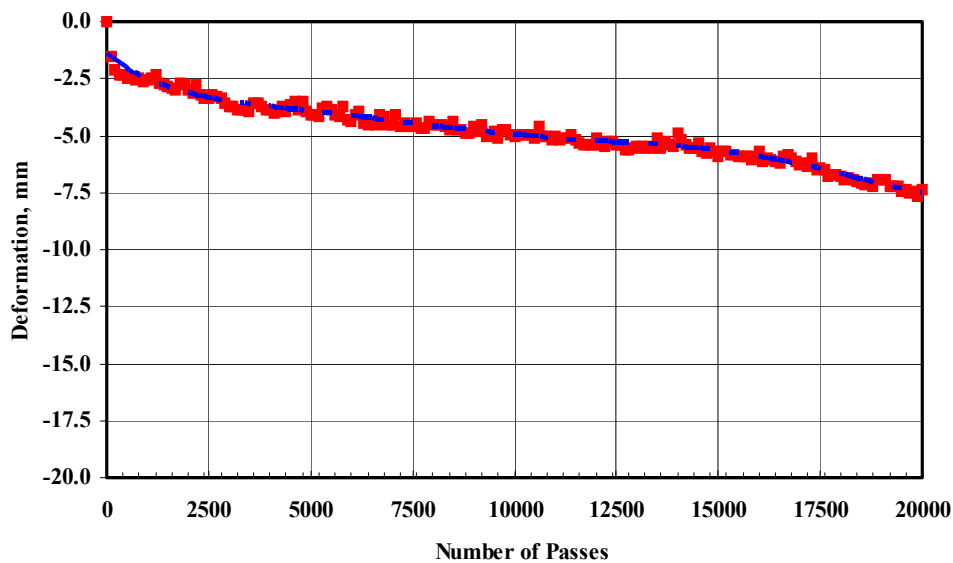
FIGURE 3   A Typical HWTD Test Result

5

Depending on the binder grade, an acceptable mix should meet the requirement suggested in Table 1. The maximum allowable deformation is 0.5 in. (12.5 mm) for all binder grades at different number of passes. According to the TxDOT specification, the maximum rut depth anywhere in the wheel path should be measured. In this study, the rut depths at the center of the two specimens were also used to assess the performance of the CRM-HMAC. In addition, tests were performed until 20,000 cycles regardless of the binder type.

TABLE 1.   TxDOT Specifications for Hamburg Wheel Tracking Device

High Temperature PG Grade	Number of Passes for Maximum Deformation of 0.5 in. (12.5 mm)
64	10,000
70	15,000
76	20,000

2.2   Static Creep Test (Tex-231-F)

This test method is used to determine the resistance to permanent deformation of bituminous mixtures at temperatures and loads similar to those experienced in the field. Measured creep properties include the total strain, permanent strain, recovered strain and slope of the steady-state portion of the creep curve. According to TxDOT, the main disadvantage of this test is that the results do not seem to be repeatable. The main advantage of this test is that it can be performed within a day with test results that correlate well with the field performance.

2.2.1   Test Procedure and Calculations for Static Creep Tests

Specimens are compacted to a density of 97 ± 1% using a Texas Gyratory Compactor (TGC). The compacted specimens, which are nominally 4 in. (100 ± 2 mm) in diameter and 2 in. (50 ± 1 mm) in height, are cooled to room temperature for a period of 24 hr. Three cycles of a 125-lb (556-N) square wave preload in one-minute intervals are applied followed by a one minute rest period for each cycle at 40°C. This allows for the loading platens to achieve a more uniform contact with the specimen. After applying the three seating loading cycles; a 125-lb (556-N) load is applied to the specimen for one hour. At the end of one hour, the load is removed to allow the specimen to rebound for 10 minutes. A typical load versus time diagram is shown in Figure 4. During the entire loading and unloading time, the load applied and the resulting vertical deformations from LVDTs are monitored and recorded. The parameters evaluated for the analysis are denoted in the Figure 5. Creep properties of a specimen, like stiffness, permanent strain and slope of the steady-state portion of creep curve, can also be determined from the plot.
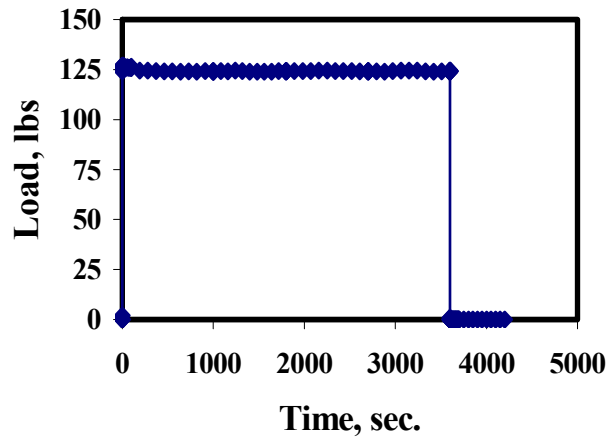
FIGURE 4   Loading Pattern for Static Creep Testing
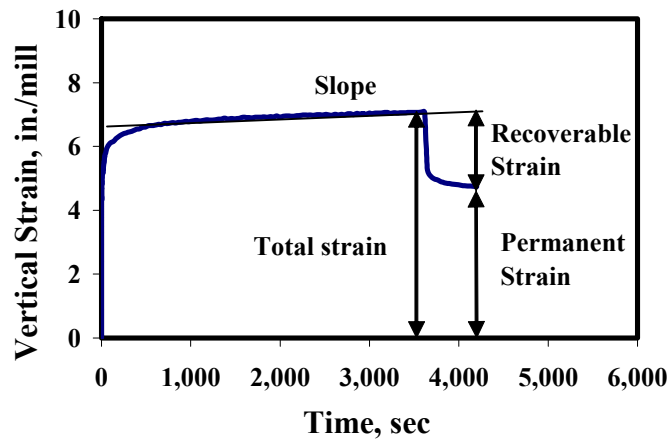
FIGURE 5   Typical Vertical Strain versus Time Plot for Static Creep Test

2.3   Dynamic Modulus Test

To mechanistically model the true behavior of a material, its fundamental properties should be measured. The response of a viscoelastic material, such as asphalt concrete, under a sinusoidal load is sinusoidal; but the response will be out-of-phase with respect to the applied load as shown in Figure 6. A phase angle (ϕ) of zero is indicative of a pure elastic material; while $\phi = 90°$ is associated with a pure viscous (Newtonian) material. A phase angle between 0° and 90° corresponds to a viscoelastic material.
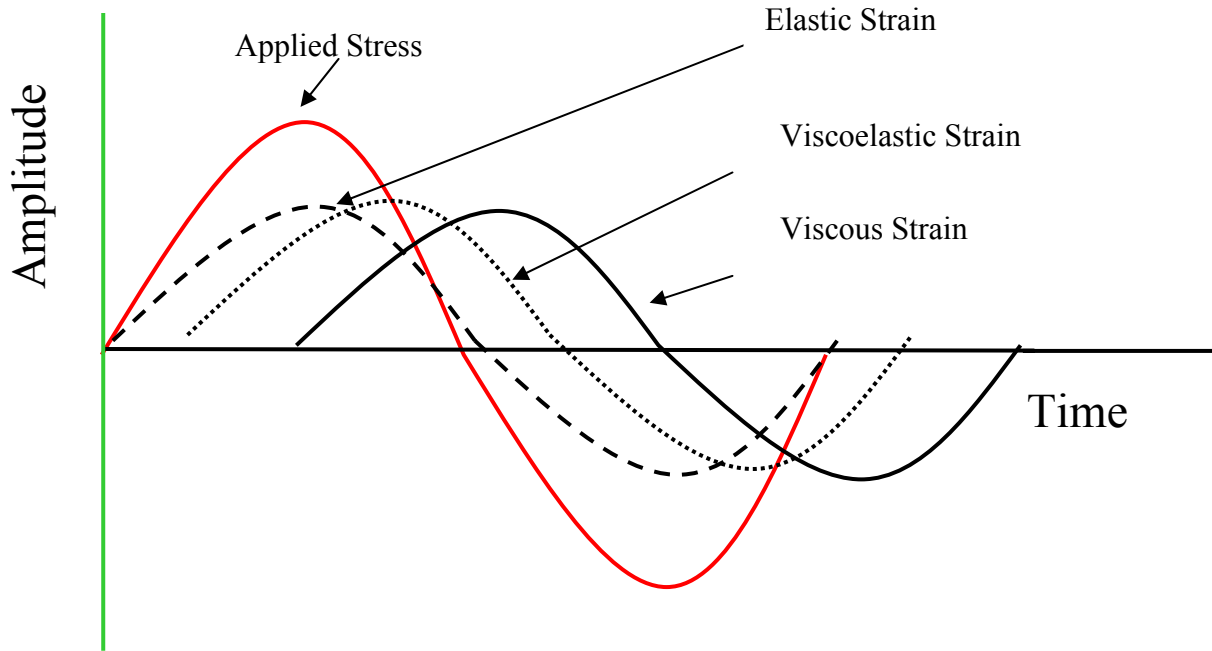
FIGURE 6   Variations in Stress and Strain with Time for Different Materials

For sinusoidal load, the applied stress and observed strain can be denoted by the following equations:

$$\sigma = \sigma_0 \sin \omega t \tag{2.1}$$

and

$$\varepsilon = \varepsilon_0 \sin (\omega t - \varphi) \tag{2.2}$$

Where:

σ = stress at time t

σ_0 = maximum applied stress

ω = angular velocity

φ = phase shift between stress and strain

ε = strain at time t

ε_0 = maximum observed strain

The complex modulus of the material, which is the ratio of the applied stress and the measured strain, can be defined as:

$$E^* = E_0 \, e^{\,j\phi} \tag{2.3}$$

where E_0 is the ratio of σ_0 and ε_0, j is the identity number and E^* is the complex modulus of the material. The absolute value of $|E^*|$ is termed as dynamic modulus.

One of the advantages of using the dynamic modulus is that the shear modulus, $|G^*|$, can be easily estimated from $|E^*|$ knowing or estimating a Poisson's ratio. Since the new asphalt binder specifications are based on the measured shear modulus, relationships between the shear moduli of asphalt binder and mixes can also be developed. In addition, the creep-compliance or stress relaxation properties can be fundamentally obtained using $|E^*|$ (Pagen, 1963). The permanent

deformation and low temperature cracking models usually utilize |E*|. Above all, the dynamic modulus measurements are used in the newly-proposed mechanistic pavement design guide.

2.3.1   Test Procedure and Calculations for Dynamic Modulus Test

The dynamic modulus test procedure is described in the test protocols submitted to the NCHRP under Project 9-19, *Superpave Support and Performance Models Management* (Witczak et al, 2002). Specimens are manufactured by coring and sawing a 4 in. (100 mm) diameter by 6 in. (150 mm) high test specimens from the middle portions of 6 in. (150 mm) by 6.5 in. (165 mm) high SGC compacted specimens. The air void content of the cored and sawed specimens should be 93 ± 1%.

The measurement setup for dynamic modulus (DM) must be rigid enough to withstand the applied cyclic loads. A hydraulic dynamic servo-valve closed-loop system manufactured by the MTS Corporation was used in this study. The schematic of the loading subsystem is shown in Figure 7. The specimen is placed on the bottom end platen, which is tightly attached to a steel base plate through a stainless steel cylinder. To minimize the vibration of the specimen, all components should be precisely machined, and custom matched.

Two linear variable differential transformers (LVDT's) are used to measure the deformation of the specimen. The positions of the LVDT's are shown in Figure 7. Two targets are fixed on one side of the specimen with a gauge length of 4 in. (102 mm) and two other targets are fixed exactly on the opposite side of the specimen. The strain experienced by the specimen is the average of the deformations on the two opposite sides of the specimen divided by the gauge length.

To measure the dynamic modulus, the test procedure and data reduction process proposed in NCRHP Project 1-37 (Standard Test Method for Dynamic Modulus of Asphalt Concrete Mixtures and Master Curves, Draft September, 2002) were adapted. Since that test procedure recommended that the strain within the specimen should be maintained within a range of 50 $\mu\varepsilon$ to 150 $\mu\varepsilon$, the applied load is adjusted for every frequency and temperature to achieve the appropriate strain level. A seating load is applied at each loading sequence in a manner that the minimum loads were never less than 5% of the maximum load.

Each specimen is tested at five temperatures: 14, 40, 73, 100 and 130°F (-10, 4, 23, 38 and 54°C). To perform the test at each temperature, the specimen is initially subjected to 200 conditioning cycles at 20 Hz. After the initial conditioning, the specimen is subjected to 50 loading cycles at 10 Hz and 5 Hz. In the end, the specimen is subjected to 7 loading cycles at frequencies of 10, 5, 2 and 1 Hz. This sequence of testing results in a total of 50 dynamic modulus tests on each specimen. To minimize the potential internal damage to the specimen, tests are performed from the lower to the higher temperatures and from the higher to lower frequencies. After each test, the data is analyzed to ensure that the strains are between 50 $\mu\varepsilon$ and 150 $\mu\varepsilon$ and that the displacements of the opposite sides of the specimen are within 15% of one

another. If the difference exceeds 15%, the specimen is discarded and a new specimen is tested. To estimate the dynamic modulus, the average amplitude of the load and the strain over the last six loading cycles are recorded. The dynamic modulus is estimated using the ratio of peak stress and peak strain.
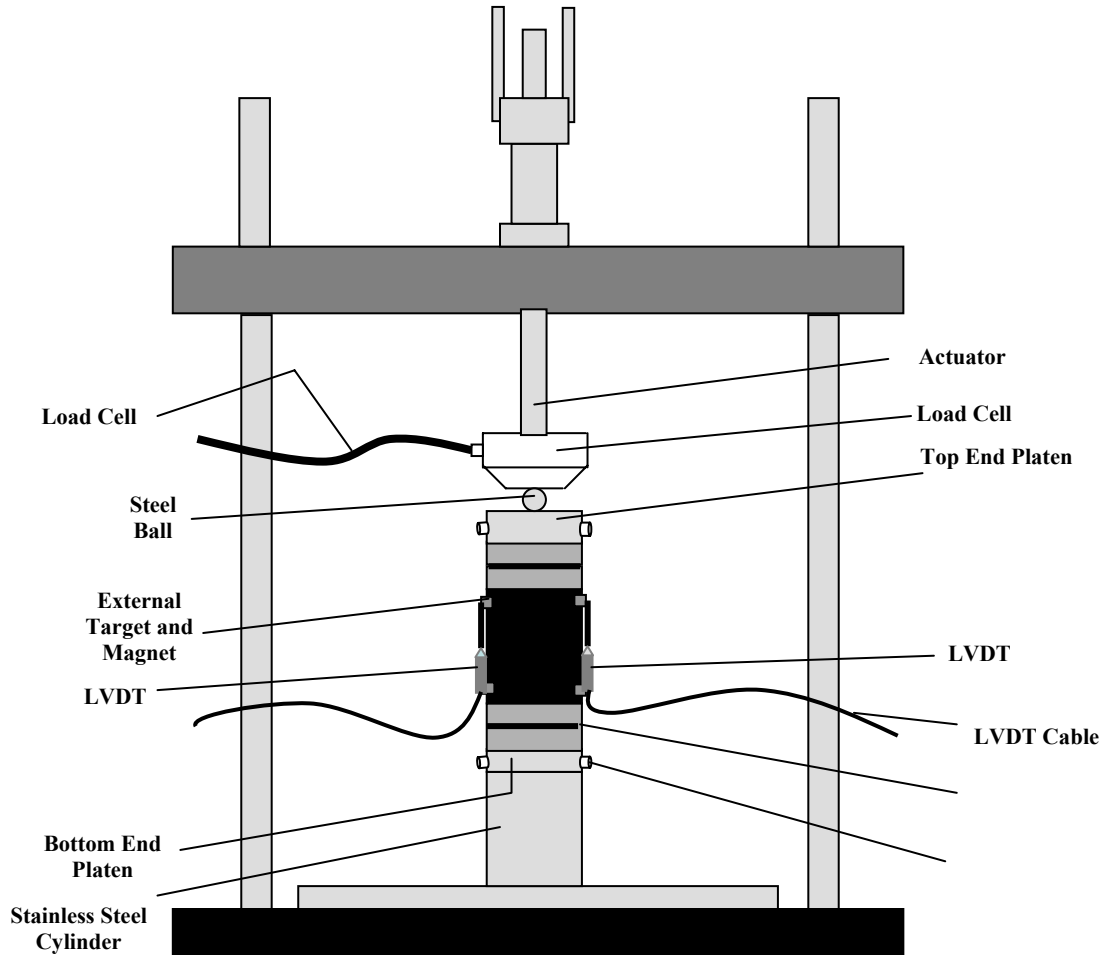
FIGURE 7   A Schematic of Dynamic Modulus Test Setup

A typical plot of measured dynamic modulus at each frequency and at different temperatures is shown in Figure 8. Assuming that the time-temperature superposition principle is valid, the moduli from each temperature are shifted horizontally to produce a master curve at a reference temperature. Typical shift factor plot is shown in Figure 9. The shifted master curve at 23°C (73°F) is shown in Figure 10. As expected, the dynamic moduli for the higher temperatures (54°C and 38°C) have to be shifted to the left while the moduli for the lower temperatures (4°C and -10°C) have to be shifted to the right to generate the master curve. The curve fitting to the
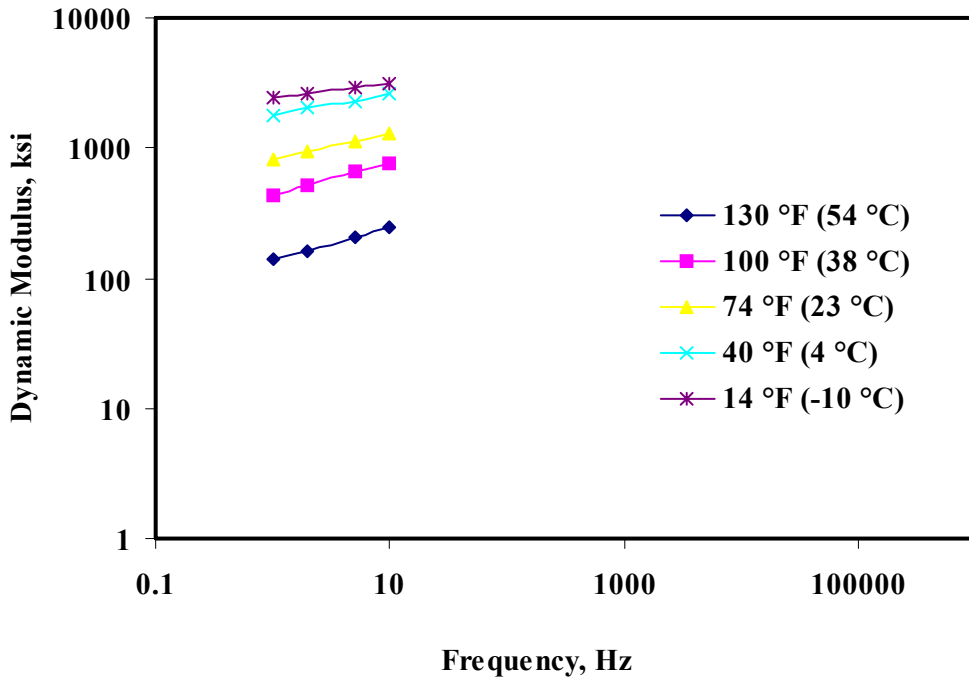
FIGURE 8   **Typical Dynamic Modulus versus Frequency Plot at Different Temperatures**
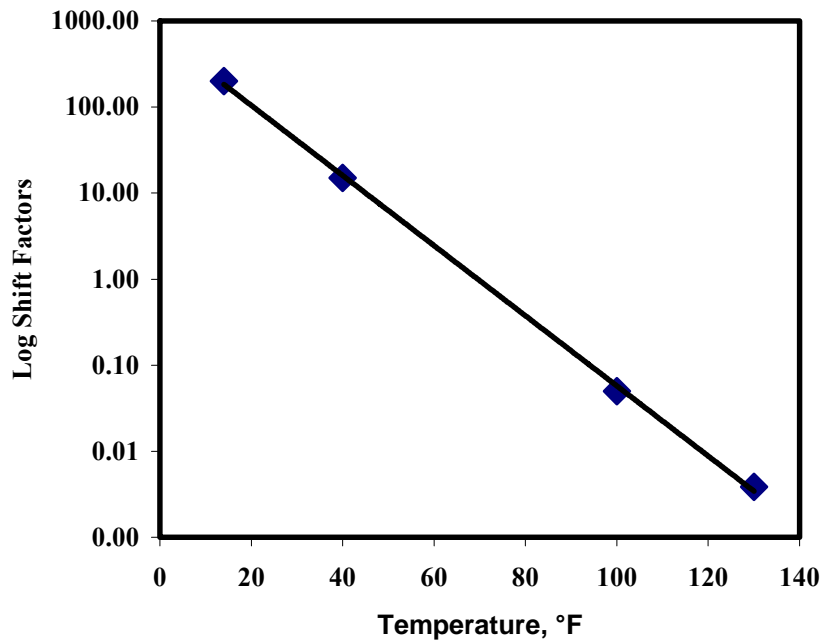
FIGURE 9   **Typical Log Shift Factor versus Temperature Plot**
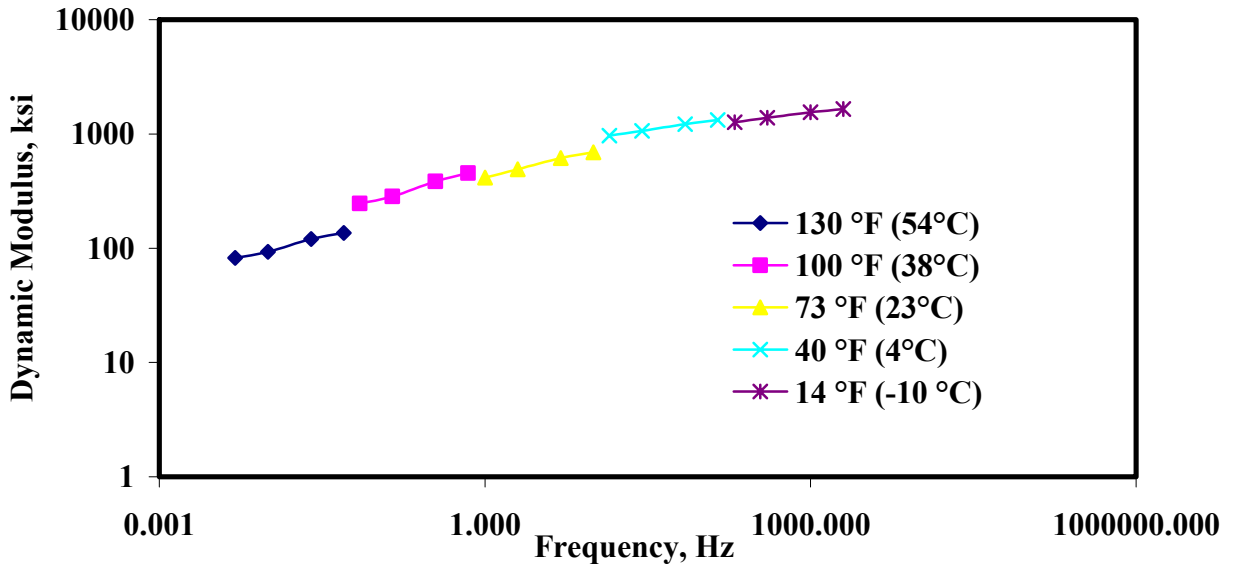
FIGURE 10   **Shifted Dynamic Modulus versus Frequency Relationship**
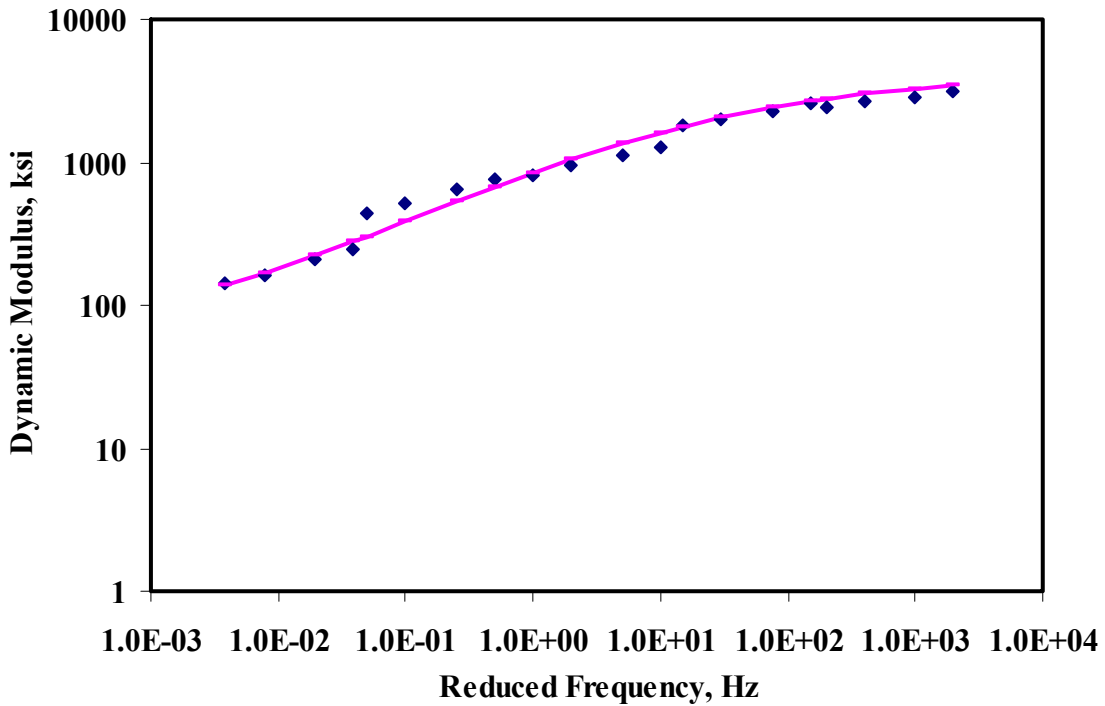
FIGURE 11   **Typical Master Curve**

master curve (Figure 11) is done by using a method developed by Pellinen and Witczak (2002). That method consists of fitting a sigmoidal curve described in Eq. 2.4 to the measured dynamic modulus test data using nonlinear least-squares regression techniques.

$$Log \ (E^*) = \delta + \frac{\alpha}{1 + e^{[\beta + \gamma \ log(\frac{1}{Hz})]}}$$

(2.4)

2.4   Flow Number Test

The flow number test is a variation of the repeated load permanent deformation test that has been used to measure the rutting potential of asphalt concrete mixtures (Roberts et al., 1996). Haversine axial compressive load pulses similar to resilient modulus are applied to the specimen. The permanent axial deformation at the end of the rest period is monitored during repeated loading and converted to strain. Witczak et al (2002) introduced the concept of flow number, which is defined as the number of load pulses when the minimum rate of change in permanent strain occurs during the repeated load test. It is determined by differentiating the permanent strain versus number of load cycles curve. The flow time test is quite appealing as a simple performance test because it is possible to use relatively simple equipment.

2.4.1   Test Procedure and Calculations for Flow Number Test

The specimen preparation process and test setup are similar to the dynamic modulus test with one exception. The deformation of specimen is monitored with the actuator LVDT rather than LVDTs mounted on the specimen. The flow number test is performed by the application of haversine axial compressive load pulses rather than sinusoidal load pulses to the specimen of 4 inch diameter and 6 inch height as shown in Figure 12a. The duration of the load pulse is 0.1 sec followed by a rest period of 0.9 sec. The test duration is about 3 hours for 10,000 loading cycles. The permanent axial deformation measured at the end of the rest period is monitored during the repeated loading (Figure 12b) and converted to strain. The recommended test protocol consists of testing the asphalt mix at one effective pavement temperature T_{eff} and one design stress level. The effective pavement temperature T_{eff} covers approximately the temperature range of 77°F (25°C) to 140°F (60°C). The design stress levels cover the range between 10 psi (69 kPa) and 30 psi (207 kPa) for the unconfined tests. Typical confinement levels range between 5 psi (35 kPa) and 30 psi (207 kPa).

In the NCHRP Project 9-19, the SPT tests results were correlated with the actual field distress for three test sites (MnRoad, WestTrack and the ALF). The flow number and flow time tests were performed at axial stresses of 10 psi and 30 psi and 100ºF and 140ºF. They found that the flow number and flow time results at a stress of 30 psi conducted at 140ºF (54ºC) correlated well with the rutting resistance of the mixtures used in the experimental sections at MnRoad, WestTrack and the ALF. Therefore, a test temperature of 140°F (54°C) and a stress level of 30 psi (210 kPa) were selected for this study.
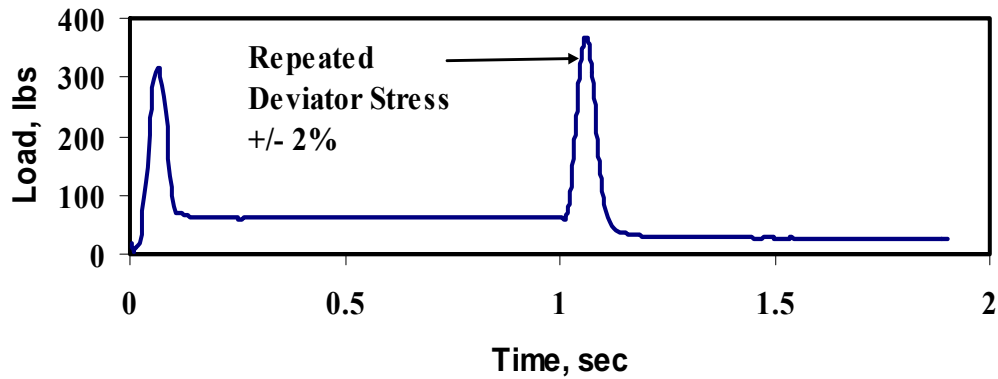
(a) Load versus Time Plot
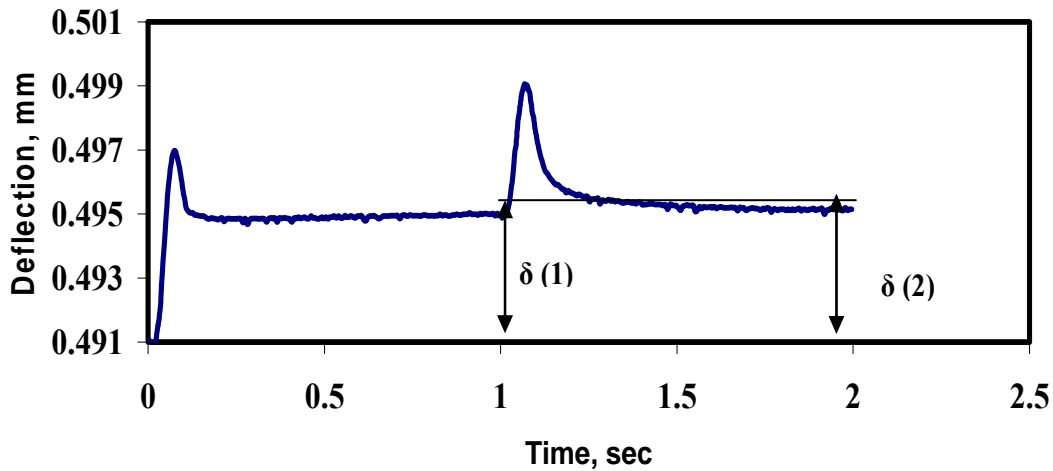
(b) Deflection versus Time Plot

FIGURE 12   Load Application and Expected Response from Flow Number Test

The results of the permanent deformation test in terms of the cumulative permanent strain versus the number of loading cycles on a log-log scale are presented in Figure 13a. The intercept *a* represents the permanent strain for the first cycle, whereas the slope *b* represents the rate of change in loading cycles. These two are derived from the linear portion of the cumulative plastic strain-repetitions relationship. The equation used to analyze these test results is

$$\varepsilon_p = aN^b$$

(2.5)

Another graph is drawn between the rate of change of axial strain and the loading cycle as shown in Figure 13b. The flow number is defined as the number of load cycles corresponding to the minimum rate of change in the permanent axial strain. In this study, the response presented in Figure 13b was used to determine the number of load cycles to failure as well.
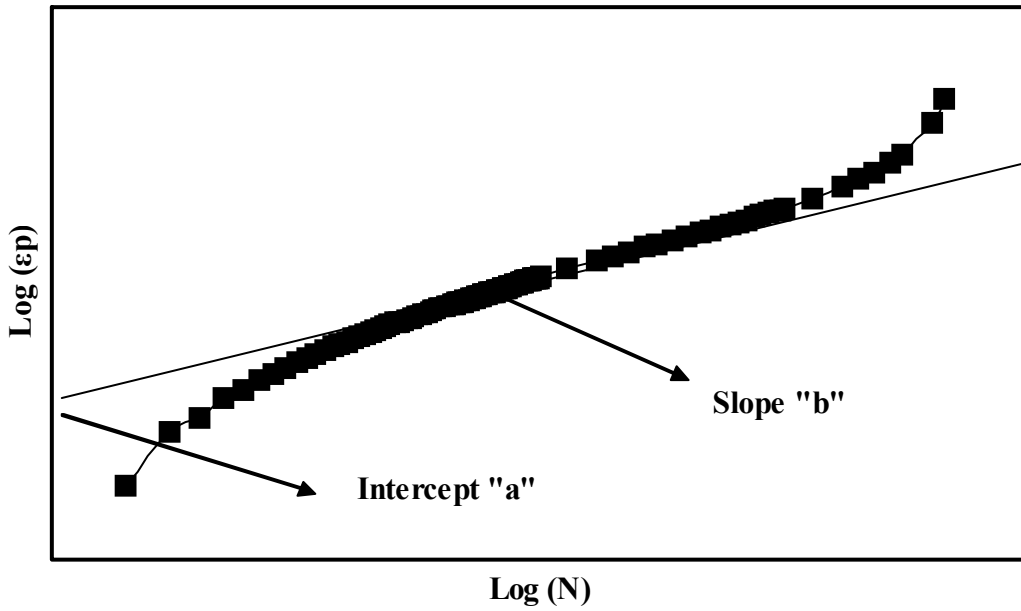
a) Regression Constants 'a' and 'b'
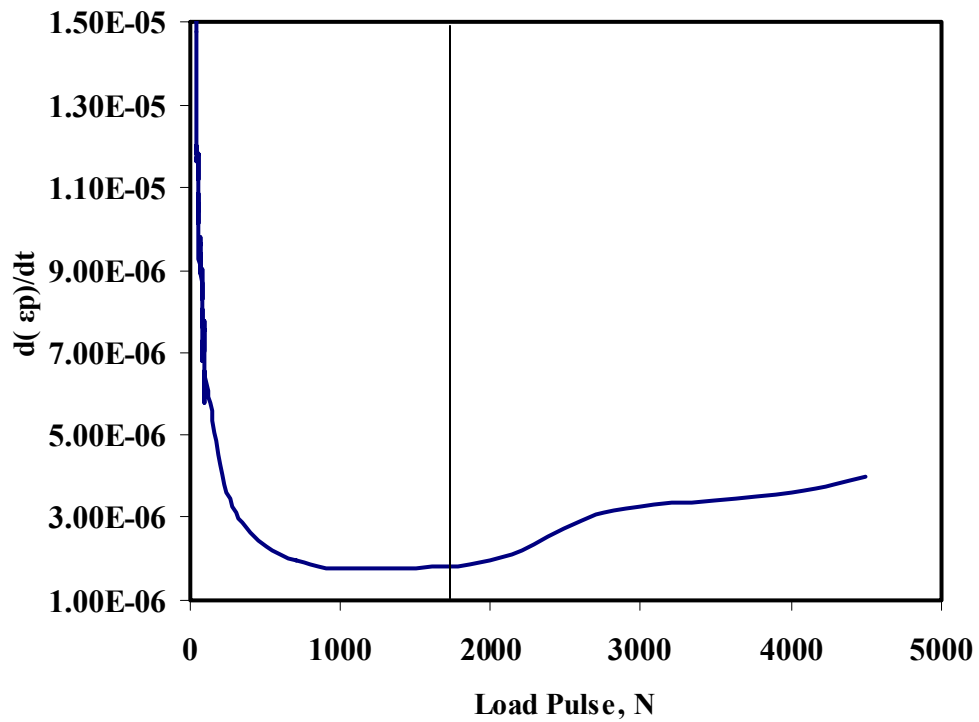
b) Rate of Change of Permanent Axial Strain versus Load Pulse

FIGURE 13   Flow Number Test Results

2.5   Flow Time Test

The modulus of a material is an important property that relates the stress to strain and is used to predict pavement distresses. For viscoelastic materials, however, it is more advantageous to use the term compliance or D(t). Compliance is the reciprocal of the modulus. The main advantage of its use in the viscoplastic theory is that the compliance allows for the separation of the time-independent and time-dependent components of the strain. In a static compressive creep test, a total strain-time relationship for a mixture is established in the laboratory under unconfined or confined condition. The static creep test, using either one load-unload cycle or incremental load-unload cycles, provides sufficient information to determine the instantaneous elastic (i.e., recoverable) and plastic (i.e., irrecoverable) components of the material response (which are time independent), as well as the viscoelastic and viscoplastic components (which are time dependent).

The flow time test is a variation of the static creep test commonly performed by TxDOT to assess the rutting potential of HMAC. In this test, a static load is applied to the specimen, and the resulting strains are recorded as a function of time. The variation introduced in the NCHRP study is the concept of flow time, which is defined as the time when the minimum rate of change in strain occurs during the creep test. The flow time is determined by differentiating the strain versus time curve. The flow time test is quite appealing as a simple performance test because the equipment is simple and the training required for its implementation is minimal. One major difference between the NCHRP and TxDOT procedures is the specimen size (4 in. by 6 in. cylinder) which may be one factor that reduces the variability of the test results as compared to the TxDOT process.

2.5.1   Test Procedure and Calculations for Flow Time Test

The specimen preparation process and test setup are similar to the flow number test setup with one exception. Tests are performed at a temperature of 140 F (54°C) and a stress level of 30 psi (210 kPa) similar to the flow number tests. However, the stress level of 30 psi is maintained for three hours rather than applying the dynamic haversine axial compressive cyclic loads.

Figure 14a shows a typical relationship between the calculated total compliance and loading time. The point at which a large increase in compliance occurs at a constant volume is defined as the flow time, which has been found to be a significant parameter in evaluating a HMAC mixture's rutting resistance. In general, power models are used to model the secondary (i.e., linear) phase of the creep compliance curve, as illustrated in Figure 14a. A common model is in the form of

$$D'(t) = D(t) - D_o = at^m \tag{2.6}$$

where,

$D'(t)$ = viscoelastic compliance component at time t,
D (t) = total compliance at time t,
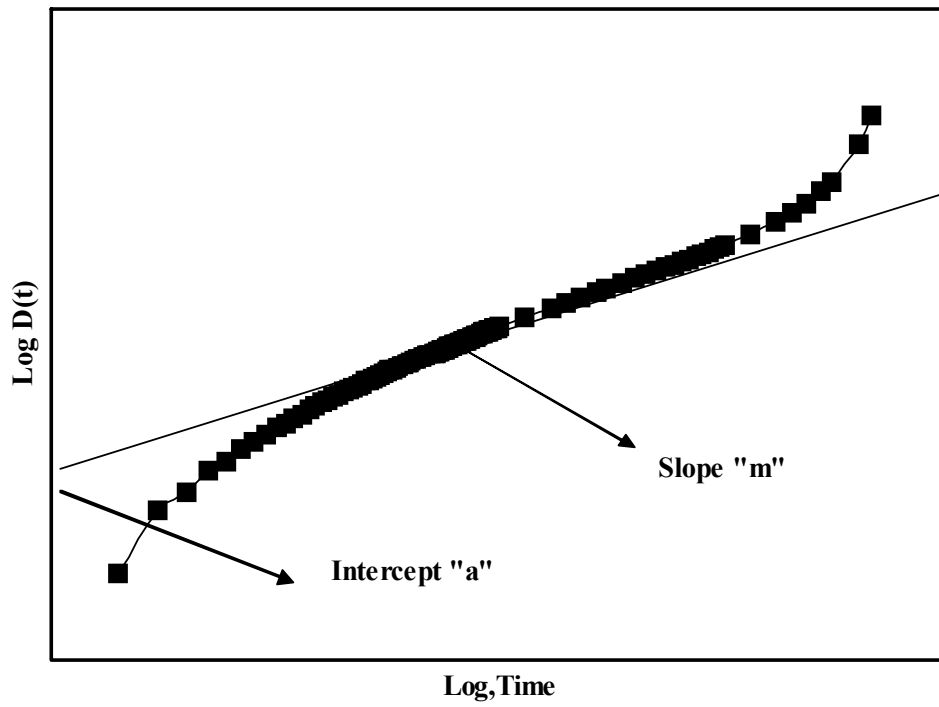
a) Regression Constant "a" and "m"
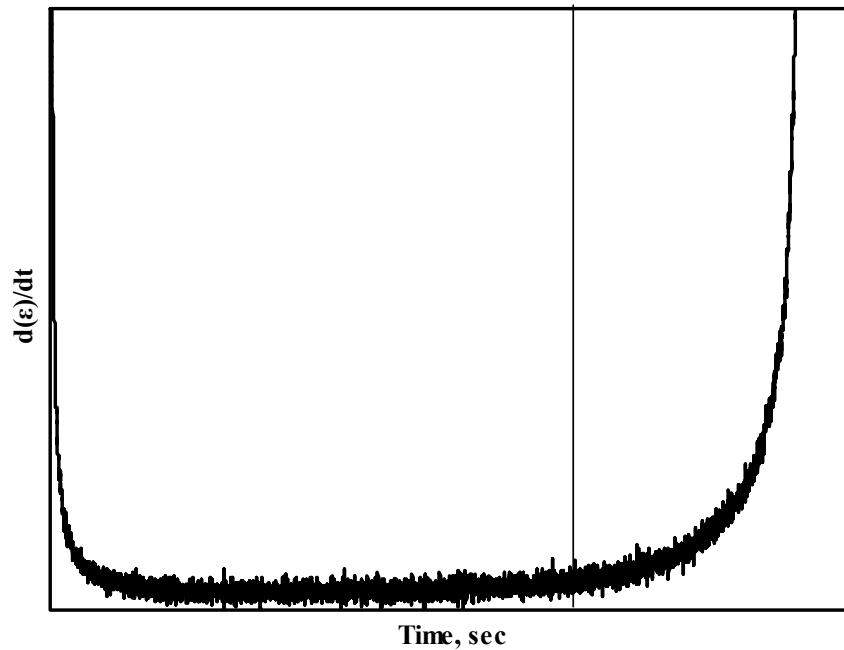
b) Rate of Change in Compliance Versus Loading Time

FIGURE 14   Flow Time Test Results

D_o = instantaneous compliance,
t = loading time, and
a, m = material regression coefficients.

The regression coefficients *a* and *m* are generally referred to as the compliance parameters. In general, the larger the value of *a* is, the larger the compliance value, D (t), the lower the modulus, and the larger the permanent deformation will be. For a constant *a*, an increase in the slope parameter *m* means a higher rate of permanent deformation.

The flow time also is viewed as the minimum point in the relationship of the rate of change of compliance to loading time, as shown in Figure 14 b. The flow time is therefore defined as the time at which the shear deformation under constant volume begins. In this study, the response presented in the Figure 14b was used to assess the failure of the mixes as well.

2.6   Indirect Tensile (IDT) Strength Test

According to Witczak et al. (2002), the indirect tensile test has been extensively used in the structural design of flexible pavements since the 1960s and, to a lesser extent, in HMA mixture design. The IDT is the test recommended for mixture characterization in the Long-Term Pavement Performance (LTPP) Program, and to support the structural design in the 1986 and 1993 AASHTO design guides. The indirect tensile test is one of the most popular tests used for the characterization of HMA mixtures. The primary reason for the test's popularity is that cores from thin lifts can be tested directly in the laboratory. Although the reliability of the indirect tensile test to detect and predict moisture damage is questionable, no other test has been found to provide consistent results at a higher reliability. In addition, SHRP recommended the use of the indirect tensile creep test method to characterize the HMA mixtures for thermal-cracking predictions.

The indirect tensile method is used to develop the tensile stresses along the diametral axis of a test specimen. The test is conducted by applying a compressive load to a cylindrical specimen through two diametrically opposed, arc shaped rigid platens. Based on the theory of elasticity, the strain can be expressed in three dimensions. Ideally, the 3-D analysis can be reduced to a 2-D analysis for special element-size and loading conditions. For the case of a circular disk, the 2-D analysis can be categorized as plane stress.

2.6.1   Test Procedure and Calculations for Indirect Tensile Test

The indirect tensile strength test is specified in test method Tex-226-F "Indirect Tensile Strength Test". The specimens are compacted to a density of 93 ± 1% using a TGC. The compacted specimens that are 4 inch in diameter and 2 inch thick are loaded diametrically at a rate of 2 inch/min. along and parallel to their vertical diametric planes. The loading configuration described develops a relatively uniform state of tensile stresses perpendicular to the load direction, which results in splitting of the specimen. In this study, tests were performed at 14°F to estimate the low temperature properties of the mixes. During the test, load and vertical

18

displacement are recorded as shown in Figure 15. A typical load vs. deformation response can be seen in Figure 16.

The recorded load at failure, P_f, is used to calculate the indirect tensile strength of the specimen using Equation:

$$\sigma_f = \frac{2P_f}{\pi d t} \tag{2.7}$$

where:
σ_f = stress at failure, which is equivalent to the indirect tensile strength,
P_f = recorded load at failure,
d = specimen diameter, and
t = specimen thickness.

Other parameters that can be obtained from the IDT strength test include the fracture energy to failure (area under the load-vertical deformation curve until maximum load) and total fracture energy (area under the load-vertical deformation curve) (Witczak et al., 2002). The fracture energy was estimated and used in this study as well.
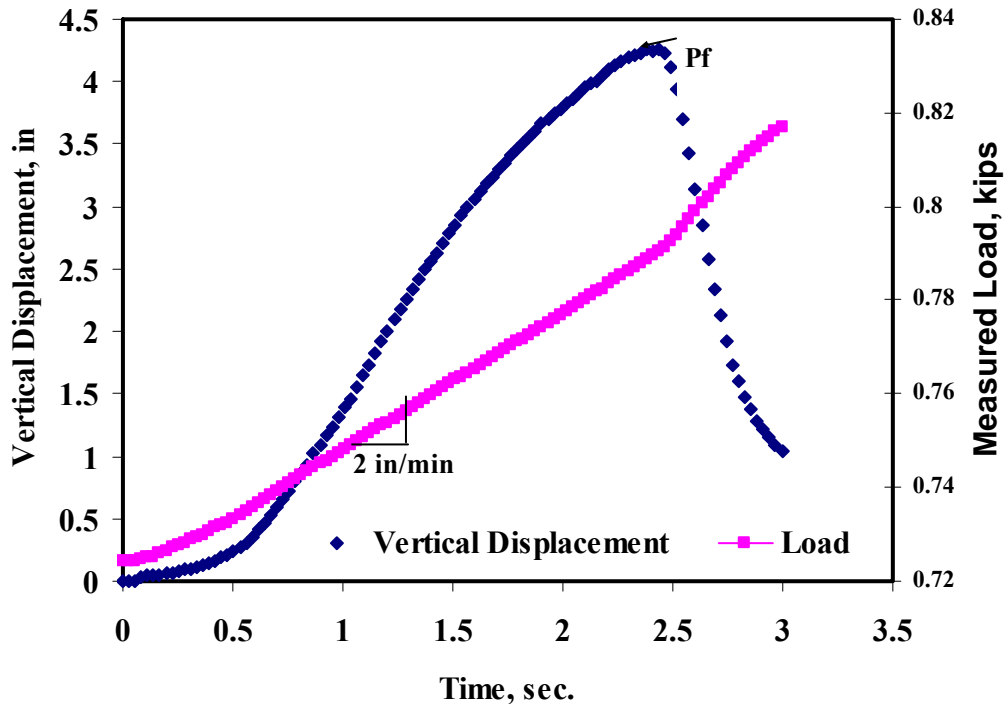
FIGURE 15   Typical Data Recorded During the IDT Strength Test

19
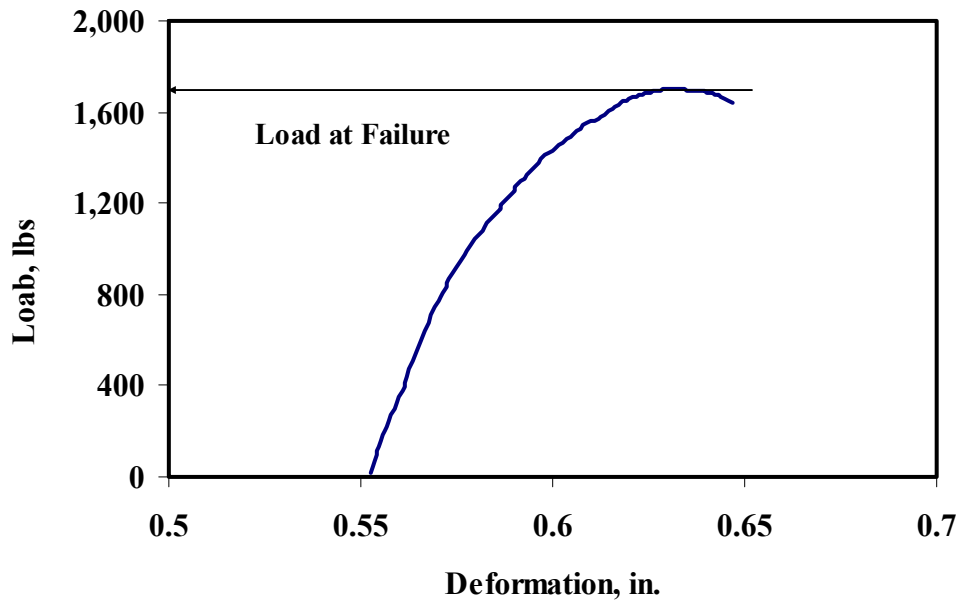
FIGURE 16   Indirect Tensile Strength Test Results (Load vs. Deformation)

2.7   Flexural Beam Fatigue Test

Load-associated fatigue cracking is one of the major distress types occurring in flexible pavement systems. The action of repeated loading caused by traffic induced tensile and shear stresses in the bound layers, which will eventually lead to a loss in the structural integrity of a stabilized layer. Fatigue cracks initiate at points where critical tensile strains and stresses occur. Additionally, the critical strain is also a function of the stiffness of the mix. Since the stiffness of an asphalt mix in a pavement varies with depth; these changes will eventually affect the location of the critical strain that causes fatigue damage. Once the damage initiates at the critical location, the action of traffic eventually causes these cracks to propagate through the entire bound layer.

Over the last 3 to 4 decades of pavement technology, it has been common to assume that fatigue cracking normally initiates at the bottom of the asphalt layer and propagates to the surface (bottom-up cracking). This is due to the bending action of the pavement layer that results in flexural stresses to develop at the bottom of the bound layer. However, numerous recent worldwide studies have also clearly demonstrated that fatigue cracking may also be initiated from the top and propagated down (top-down cracking). This type of fatigue is not as well defined from a mechanistic viewpoint as the more classical "bottom-up" fatigue. In general, it is hypothesized that critical tensile and/or shear stresses develop at the surface and cause extremely large contact pressures at the tire edges-pavement interface. This scenario, coupled with highly-aged (stiff) thin surface layer that have become oxidized, is felt to be responsible for the surface cracking. To characterize fatigue in asphalt layers, numerous models can be found in the existing literature. The most common model used to predict the number of load repetitions to fatigue cracking is a function of the tensile strain and mix stiffness (modulus). The basic

20

structure for almost every fatigue model developed and presented in the literature for fatigue characterization is of the following form

$$N_f = K_1 \left(\frac{1}{\varepsilon_t}\right)^{K_2} \left(\frac{1}{E}\right)^{K_3} = K_1 (\varepsilon_t)^{-K_2} (E)^{-K_3} \tag{2.8}$$

where:
  N_f = number of repetitions to fatigue cracking
  ε_t = tensile strain at the critical location
  E = stiffness of the material
  K_1, K_2, K_3 = laboratory calibration parameters

In the laboratory, two types of controlled loading are generally applied for fatigue characterization: constant stress and constant strain. In constant stress testing, the applied stress during the fatigue testing remains constant. As the repetitive load causes damage in the test specimen, the strain increases resulting in a lower stiffness with time. In the case of the constant strain test, the strain remains constant with the number of repetitions. Because of the damage due to repetitive loading, the stress must be reduced resulting in a reduced stiffness as a function of repetitions. The constant stress type of loading is considered applicable to thicker pavement layers usually more than 8 inches while constant strain of loading is considered applicable to thinner pavements usually less than 4 in. (SHRP-A-404). For AC thicknesses between these extremes, fatigue behavior is governed by a mixed mode of loading, mathematically expressed as some model yielding intermediate fatigue prediction to the constant strain and stress conditions.

2.7.1   Test Procedure and Calculations for Flexural Beam Fatigue Test

Flexural fatigue tests are performed according to the AASHTO TP8 and SHRP M-009 (Standard Method of Test for Determining the Fatigue Life of Compacted Bituminous Mixtures Subjected to Repeated Flexural Bending). The flexural fatigue test has been used by various researchers to evaluate the fatigue performance of pavements (SHRP-A-404, 1994; Harvey and Monismith, 1993; Tayebali et al., 1995; Witczak et al., 2001). Figure 17 shows a flexural fatigue apparatus. The device is typically placed inside an environmental chamber to control the temperature during the test.

The cradle mechanism allows for free translation and rotation of the clamps and provides loading at the third points as shown in Figure 18. Pneumatic actuators at the ends of the beam center it laterally and clamp it. Servomotor driven clamps secure the beam at four points with a pre-determined clamping force. Haversine or sinusoidal loading may be applied to the beam via the built-in digital servo-controlled pneumatic actuator. A "floating" on-specimen transducer measures and controls the true beam deflection irrespective of loading frame compliance. The test is run under either a controlled strain or a controlled stress loading.

In the constant stress mode, the stress remains constant but the strain increases with the number of load repetitions. In the constant strain test, the strain is kept constant and the stress decreases with the number of load repetitions. In either case, the initial deflection level is adjusted so that

the specimen will undergo a minimum of 10,000 load cycles before its stiffness is reduced to 50% or less of the initial stiffness.

FIGURE 17   Flexural Fatigue Test Apparatus
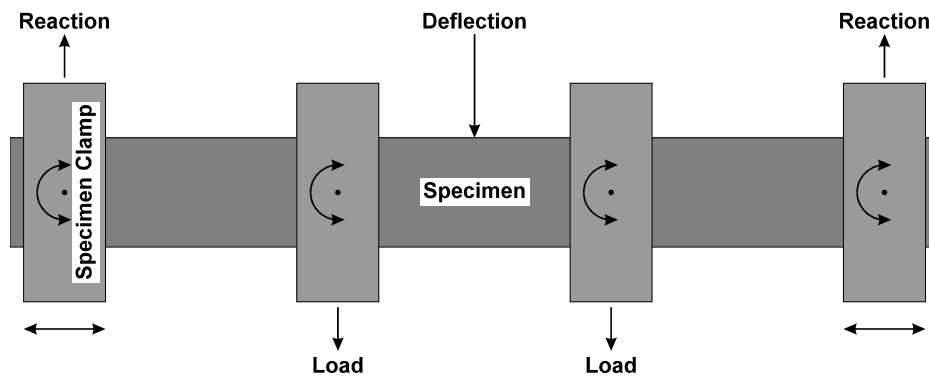
FIGURE 18   Loading Characteristics of the Flexural Fatigue Apparatus

In this study, all tests were conducted in the control strain type of loading. In summary the following conditions were used:

Load condition: Constant strain level, minimum of 5 levels in the range of 300-1900 $\mu\varepsilon$
Load frequency: 10 Hz
Test temperature: 40, 70, and 100°F (4.4, 21, and 37.8°C)

The initial flexural stiffness is measured at the 50th load cycle. Fatigue life or failure under control strain is defined as the number of cycles corresponding to a 50% reduction in the initial stiffness. The loading on most specimens is extended to reach a final stiffness of 30% of the initial stiffness instead of the 50% as required by AASHTO TP8 and SHRP M-009. The control and acquisition software load and deformation data are reported at predefined cycles spaced at logarithmic intervals.

The test utilized in this study applied repeated third-point loading cycles as shown in Figure 18. The maximum tensile stress and maximum tensile strain were calculated as:

$$\sigma_t = 0.357 \, P \, / \, b \, h^2 \tag{2.9}$$

$$\varepsilon_t = 12 \, \delta \, h \, / \, (3 \, L^2 - 4 \, a^2) \tag{2.10}$$

where,
σ_t = Maximum tensile stress
ε_t = Maximum tensile strain
P = Applied load
b = Average specimen width
h = Average specimen height
δ = Maximum deflection at the center of the beam
a = Space between inside clamps
L = Length of beam between outside clamps,

The flexural stiffness was calculated as follow.

$$E = \sigma_t \, / \, \varepsilon_t \tag{2.11}$$

where E = Flexural stiffness.

The phase angle (ϕ) in degrees was determined as follow.

$$\phi = 360 \, f \, s \tag{2.12}$$

where,
 f = Load frequency, Hz
 s = Time lag between P_{max} and δ_{max}, seconds

The dissipated energy per cycle and the cumulative dissipated energy were computed using Equations 2.13 and 2.14, respectively.

$$w = \pi \, \sigma_t \, \varepsilon_t \, \sin \phi \tag{2.13}$$

$$\text{Cumulative Dissipated Energy} = \sum_{i=1}^{i=N} w_i \tag{2.14}$$

where,
 w = Dissipated energy per cycle
 w_i = w for the ith load cycle

During the test, the flexural stiffness of the specimen was determined after each load cycle. The stiffness of the beam was plotted against the load cycles; the data was best fitted to an exponential function following the form of.

$$E = E_i \, e^{bN} \tag{2.15}$$

where,

        E = Flexural stiffness after n load cycles
        E_i = Initial flexural stiffness
        e = Natural logarithm to the base e
        b = Constant
        N = Number of load cycles

Once Equation 2.15 was formulated, the initial stiffness S_i can be obtained. Failure was defined as the point at which the specimen stiffness is reduced to 50 percent of the initial stiffness. The number of load cycles at which failure occurred was computed by solving Equation 2.15 for N, or simply:

$$N_{f,50} = [\ln (E_{f,50} / E_i)] / b \qquad\qquad (2.16)$$

where,

$N_{f,50}$ = Number of load cycles to failure
$E_{f,50}$ = Stiffness at failure

The AASHTO TP8-94, and SHRP M-009, flexural fatigue testing protocol, require preparation of oversize beams that later have to be sawed to the required dimensions. The final required dimensions are $15 \pm 1/4$ in. (380 ± 6 mm) in length, $2 \pm 1/4$ in. (50 ± 6 mm) in height, and $2.5 \pm 1/4$ in. (63 ± 6 mm) in width. The procedure does not specify a specific method for preparation. Several methods have been used to prepare beam molds in the laboratory including full-scale rolling wheel compaction, miniature rolling wheel compaction, and vibratory loading.

In this study, beams were prepared using a vibratory loading applied by a servo-hydraulic loading machine. A beam mold was manufactured at ASU with structural steel that is not hardened. The mold consists of a cradle and two side plates as shown in Figure 19. The inside dimensions of the mold are 1/2 inch (12 mm) larger than the required dimensions of the beam after sawing in each direction to allow for a 1/4 inch (6 mm) sawing from each face. A top loading platen was originally connected to the loading shaft assembly in the middle as shown in Figure 20. The top platen is made of a series of steel plates welded at the two ends to distribute the load more evenly during compaction. The loading shaft was connected to the upper steel plate rather than extending it to the bottom plate so that the load can be distributed more uniformly. If the bottom surface of the bottom plate is machined to be slightly concave upward, it would counter balance any bending that might occur during compaction and produce more uniform air void distribution.

FIGURE 19   Manufactured Mold for Beam Compaction and Compacted Specimens.

FIGURE 20   Top Loading Platen for Compaction of Fatigue Specimens

2.8   Ultrasonic Testing

The ultrasonic device is a portable seismic device which measures travel time of pulses of seismic waves through a material. The seismic waves are generated by a built-in pulse generator, which transforms an electrical pulse to a mechanical vibration through a transducer. The seismic wave arrival time is recorded by a receiver, which is connected to an internal clock. The internal clock has the capability of automatically measuring and displaying the travel time of the waves. The travel time and the density of the specimen are used to determine the moduli of the HMAC specimens. The main advantage of this test is that it is a nondestructive test. In addition, the tests can be performed on the laboratory-prepared specimens as well as field cores. Another advantage is that the modulus measured can be combined with dynamic modulus curve to develop field acceptance criterion.

2.8.1   Test Procedure and Calculations for Ultrasonic test

The specimens prepared for any of the tests described above can be used to perform ultrasonic tests. The ultrasonic laboratory setup used in this study is shown in Figure 21. The elastic

FIGURE 21   Ultrasonic Test Device for HMAC Specimens

modulus of a specimen is measured using an ultrasonic device containing a pulse generator and a timing circuit, coupled with piezoelectric transmitting and receiving transducers. The dominant frequency of the energy imparted to the specimen is 54 kHz. The timing circuit digitally displays the time needed for a wave to travel through a specimen. To ensure full contact between the transducers and a specimen, special removable epoxy couplant caps are used on both transducers. To secure the specimen between the transducers, a loading plate is placed on top of it, and a spring-supporting system is placed underneath the transmitting transducer. The receiving transducer, which senses the propagating waves, is connected to an internal clock of the device. The clock automatically displays the travel time, t_v that can be used to calculate the constrained modulus, M_V, as:

$$M_v = \rho V_P^2 = \rho(\frac{L}{t_V})^2 \tag{2.17}$$

where:
ρ = density
V_p = compression wave velocity
L = average length of the specimen

This equation may be simplified to:

$$M_V = \frac{4mL}{\pi d^2 t_V^2} \tag{2.18}$$

where,
m = mass of the specimen
d = average diameter of the specimen.
Young's Modulus, E_v, may be determined from:

26

$$E_V = M_V \left[\frac{(1-2v)(1+v)}{(1-v)} \right] \qquad (2.19)$$

The Poisson's ratio, v, can be assumed based on experience.

2.9 Specimen Preparation

The specimens for the Dynamic Modulus, Flow Time and Flow Number tests were prepared in accordance with the Superpave mix design. Mixing was done with a mechanical mixer. After mixing, the loose materials were subjected to the short-term aging in a forced-draft oven at a constant temperature equal to the mixing temperature. For the CRM-HMAC mixes, the short-term aging period was 2 hours as recommended by TxDOT. During the short-term aging period, the loose mix was stirred every hour to ensure a uniform aging. To minimize damage to the specimens during compaction, the compaction temperature of 400 ^{o}F was used. This temperature was selected based on the viscosity-temperature relationship presented in Appendix A. The loose mix was compacted into 6-in. diameter by 7-in. high specimens using the Superpave Gyratory Compactor (SGC). The compacted specimens were cooled to room temperature for a period of 24 hr, and then cored and saw cut to a diameter of 4 inches and a height of 6 inches. The air void content of each specimen was measured using the CoreLok device to ensure a density of 93 ± 0.5%. The specimens for the Hamburg Wheel Tracking Device (HWTD) tests were prepared as per modified compaction method included in Appendix B using an SGC, for the Indirect Tensile Strength tests as per test method Tex-226-F using TGC, and for the Static Creep tests as per Tex-231-F using a TGC.

For the beam fatigue tests, the asphalt rubber mixtures were heated for two hours at 325°F (163°C). The mold was heated separately for one hour at the same temperature as the mix. The mixture was placed in the mold in one load. The mold was then placed on the bottom plate of the loading machine and the top platen was lowered to contact the mixture. A load of 0.2 psi (1.4 kPa) was applied to seat the specimen. A stress-controlled sinusoidal load with a frequency of 2 Hz and a peak-to-peak stress of 400 psi (2.8 MPa) was then applied to compact the specimen. Since the height of the specimen after compaction was fixed, the weight of the mixture required to reach a specified air void content was pre-calculated. Knowing the maximum theoretical specific gravity and the target air voids, the weight of the mixture was determined. During compaction, the loading machine was programmed to stop when the required specimen height was reached.

After compaction, specimens were left to cool to ambient temperature, and were brought to the required dimensions for fatigue testing by sawing 1/4 inch (6 mm) from each side. The specimens were cut using a water-cooled saw to the standard dimension of 2.5 in. (63.5 mm) wide, 2.0 in. (50.8 mm) high, and 15 in. (381 mm) long. Finally, the air void content was measured by using the saturated surface-dry procedure Tex-207-F (AASHTO T166, Method A) for the conventional mixture.

CHAPTER 3   SELECTION OF MATERIAL AND PERFORMANCE TEST RESULTS

To identify a reliable test that can accurately characterize the CRM-HMAC, the performance of several mixes needed to be evaluated using the conventional TxDOT test procedures as well as the recently-developed simple performance tests (dynamic modulus, flow number and flow time). For this purpose, four different mixes were selected. The mix-selection and the performance evaluation test results are documented in this chapter.

3.1   Selected Material

To achieve the objective of identifying a suitable performance test, both plant-produced and laboratory-produced mixes were used. In total, four mixes were selected for the performance evaluation. Three of the mixes were plant-produced while one was laboratory-produced. The historical performance of the two of the plant-produced mixes had been well documented, while one of the mixes had been recently placed and its performance was not known at this point. The fourth mix was produced in the laboratory; therefore, its performance was also unknown. The mix design and relevant information for each mix are included in Table 2. The mixes with known field performance were obtained from two construction projects in the Odessa District. The mixes with no field performance history were obtained from the El Paso District. One of the mixes was designed and prepared at UTEP using a modified version of Tex-232-F procedure proposed by Swami et al. (2005), while the other one was obtained from construction site.

The two plant-produced mixes from Odessa have been designated as Plant Mix (RA) and Plant Mix (J). Both mixes had similar base asphalt type (AC-10) and similar coarse aggregate types. The main differences between the two were the asphalt content and the source of screenings. The Plant Mix (J) had an asphalt content of 8.5% with Odessa Screenings while the Plant Mix (RA) had asphalt content 7.8% with Bolmorhea Screenings.

According to the Odessa District, both mixes have historically performed well over the years. However, the recently placed Plant Mix (J) had shown signs of distress approximately 1 year after placement. The reason for the failure was attributed to the variation between the gradations of the in-place and laboratory mixes. The ignition oven test results of the mix are shown in Table 2. The percentage of material passing No. 4 sieve differed from the JMF. The expected percent passing No. 4 sieve size was 47%, while more than 58% of the materials retrieved from the site passed through that sieve. The Plant Mix (RA) had been performing well over the years and had shown no signs of distress, therefore, the laboratory performance test results should identify Plant Mix (RA) to be a well performing mix.

TABLE 2.   CRM-HMAC Mixes Evaluated for Selection of Suitable Performance Test

Identification	Plant Mix (RA)		Plant Mix (J)		Plant Mix (JC)		Lab Mix (U)	
Aggregate Types	• Grade 4 • Type D • Odessa Screenings		• Grade 4 • Type D • Odessa (Balmorhea)		• Red 3/8, • McK "3/8" • McK Fine Screenings		• Red 3/8, • McK "3/8" • McK Fine Screenings	
Base Binder Grade	AC-10		AC-10		PG 64-22		PG 64-22	
	Lab Design	Plant Produced	Lab Design	Plant Produced	Lab Design	Plant Produced	Lab Design	Plant Produced
Binder Content, %	7.8	7.5	8.5	8.4	7.5	7.1	8.5	N/A
Gradation, % passing **Sieve Size, mm**								
9.5	99.0	99.0	99.3	99.0	96.1	100.0	100.0	N/A
4.75	49.2	52.0	47.1	58.0	45.0	61.0	39.1	N/A
2.0	19.3	27.0	20.2	27.0	19.3	26.0	8.2	N/A
0.425	9.4	15.0	9.0	12.0	8.9	11.0	5.5	N/A
0.180	6.9	-	6.1	-	6.7	-	4.8	N/A
0.075	5.0	3.0	4.3	0.0	5.1	6.0	4.3	N/A
Maximum Specific Gravity (G_{mm})	2.305	2.305	2.301	2.301	2.400	2.425	2.404	N/A
Rubber, %	17.5	N/A	18.0	N/A	16.0	N/A	18.0	N/A

The plant-produced mix from El Paso and the laboratory-produced mix at UTEP are designated as Plant Mix (JC) and Lab Mix (U), respectively. Both mixes contained similar base asphalt (PG64-22) and similar aggregates. The main differences between the two mixes are the asphalt content and CRM content. The Plant mix (JC) contained an asphalt content of 7.5% with 16% CRM while the Lab Mix (U) contained an asphalt content of 8.5% with 18% CRM. The Lab Mix (U) was designed using the proposed modified Tex-232-F by Swami et al. (2005), while the Plant Mix (JC) was designed using the existing Tex-232-F. The ignition oven test results of the Plant Mix (JC) identified a lower asphalt content and more material passing No. 4 sieve in comparison to the mix design submitted to TxDOT for approval. Since performance of the two mixes is unknown, the results from the performance tests can be used for future validation.

3.2 Results and Discussion of Performance Testing

The performance evaluation test results of the four mixes are included in the following sections. The goal all along was to perform each of the performance tests on triplicate specimens. In some cases, this was not possible due to the shortage of the materials as the material required for modification of Tex-232-F was more than expected.

3.2.1 Hamburg Wheel Tracking Device (HWTD) Test Results

The HWTD tests were performed in accordance with the TxDOT procedure, which suggests preparing four identical cylindrical specimens and sawing them at the edge as shown in Figure 22. Two sawed specimens were placed along the left wheel path and the other two along the right wheel path. The two specimens placed on each side were considered to be one specimen. The maximum rutting depth observed in the combined specimens on each wheel path was averaged to estimate the rutting potential of a mix. Although the maximum rutting depth can be anywhere on the combined specimens, it usually occurs in the centre of the combined specimens (referred to as "Center of Slab" in Figure 22). This can be attributed to the minimal confinement around the central area.

For this study, it was decided to record permanent deformations at three different locations. The first location was selected to be the center of each specimen and is designated at center of specimen in Figure 22. For this location, the deformation from the center of each specimen was averaged for each wheel and is reported as the deformation observed at the center of specimen. The advantage of measuring the deformation at this location is that only two specimens can be tested to assess the field performance of a HMAC rather than four specimens. The second location was selected to be at the interface of the two specimens (as shown in Figure 22) and is reported as deformation observed at the center of the slab. In addition, the maximum deformation observed at any location along the wheel path (along center line) was also recorded and reported as the maximum deformation observed (Tex-242-F procedure suggests to report this number).
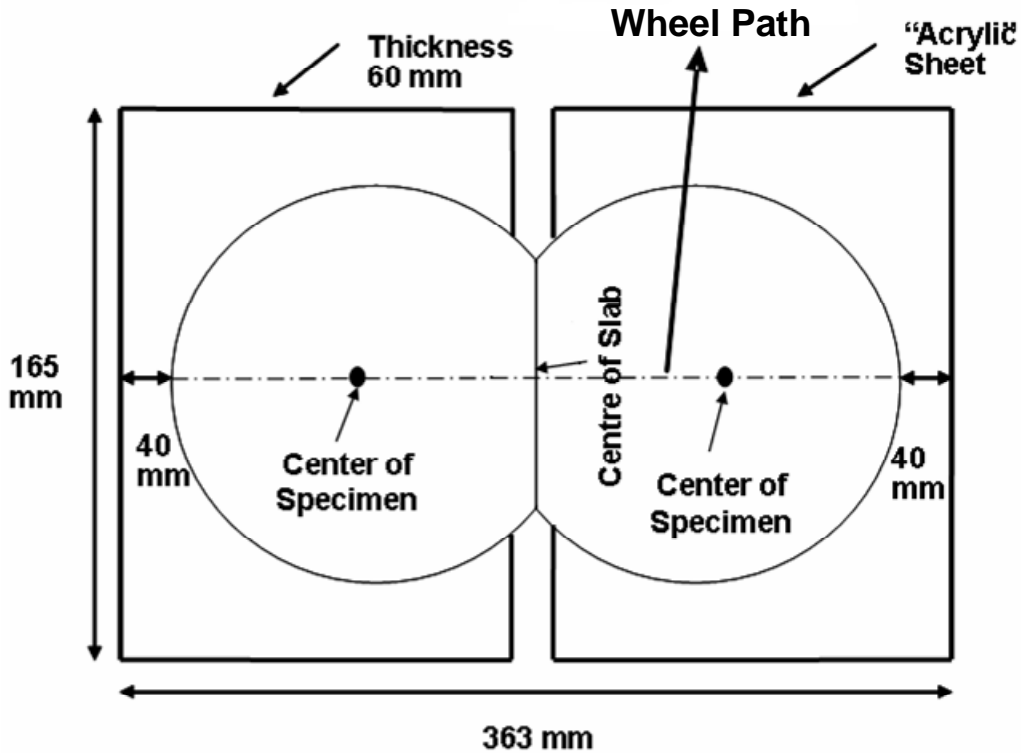
FIGURE 22   HWTD Specimen Setup

In addition, the deformations were collected more frequently so that a nth-degree polynomial can be fitted to them more reliably. A typical test result for Plant Mix (J) along with the sixth-degree polynomial and the associated regression coefficients are shown in Figure 23. The coefficient of determination of 0.97 indicates that the best-fit curve describes the measured data well. One drawback of the polynomial curve shown in Figure 23 is that it does not fit the rut from the initial (first 500) passes well. Since the main focus of the HWTD test is to determine the rut at the end of the 10,000 or higher passes, the initial portion of the rut curve is of no significance. To represent the results more clearly, only the best-fit curves are plotted and described from now on.

The HWTD test results for the four mixes are shown in Figures 24 through 26. As per test method Tex-242-F, the variation in rut depth measured with the number of passes for each mix is shown in Figure 24. The Plant Mix (RA) and Plant Mix (JC) rutted less than 0.20 in. (5 mm) while the Plant Mix (J) and Lab Mix (U) deformed less than 0.5 in. (12.5 mm). Since the Plant Mix (J) and Lab Mix (U) contained higher asphalt contents, such a trend is anticipated. At the center of the slab (Figure 25) and center of specimen (Figure 26), the observed rut depths were less than 0.3 in. (7.5 mm) as well. From the test results, all mixes met the TxDOT requirement of less than 0.5 in. deformation at the end of 20,000 cycles independent of the location of the measured deformation.

$$y = 7E\text{-}24x^6 - 4E\text{-}19x^5 + 1E\text{-}14x^4 - 1E\text{-}10x^3 + 8E\text{-}07x^2 - 0.0027x - 1.4647$$

$$R^2 = 0.9781$$
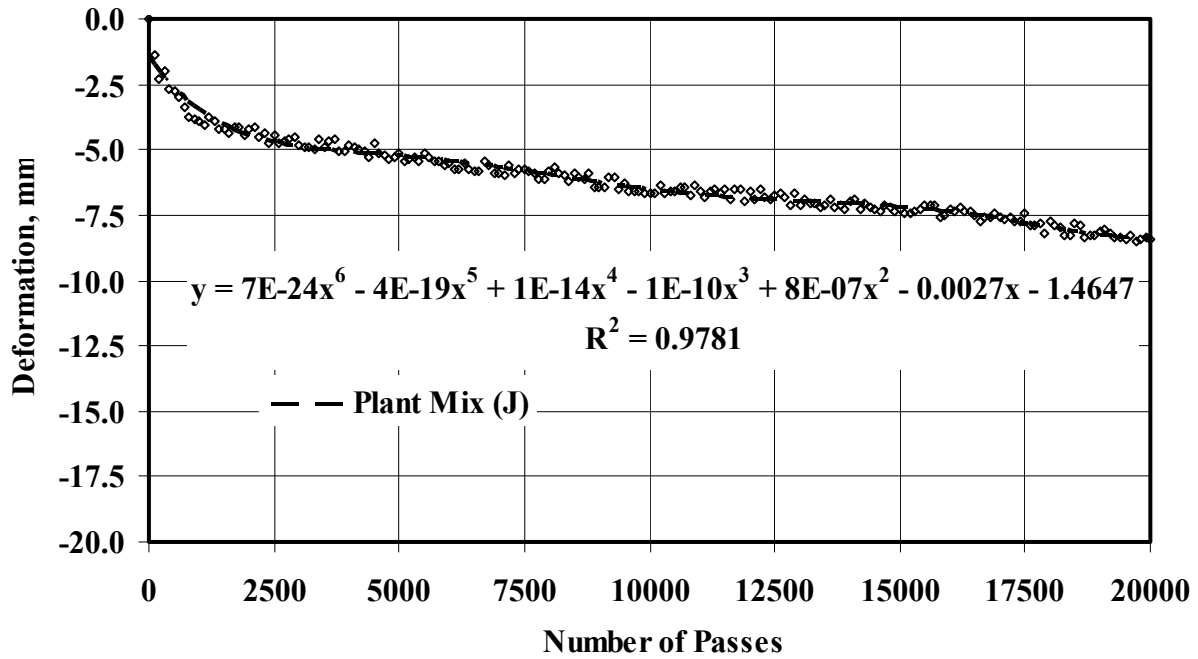
FIGURE 23   HWTD Test Results for Plant Mix (J) at Maximum Deformation
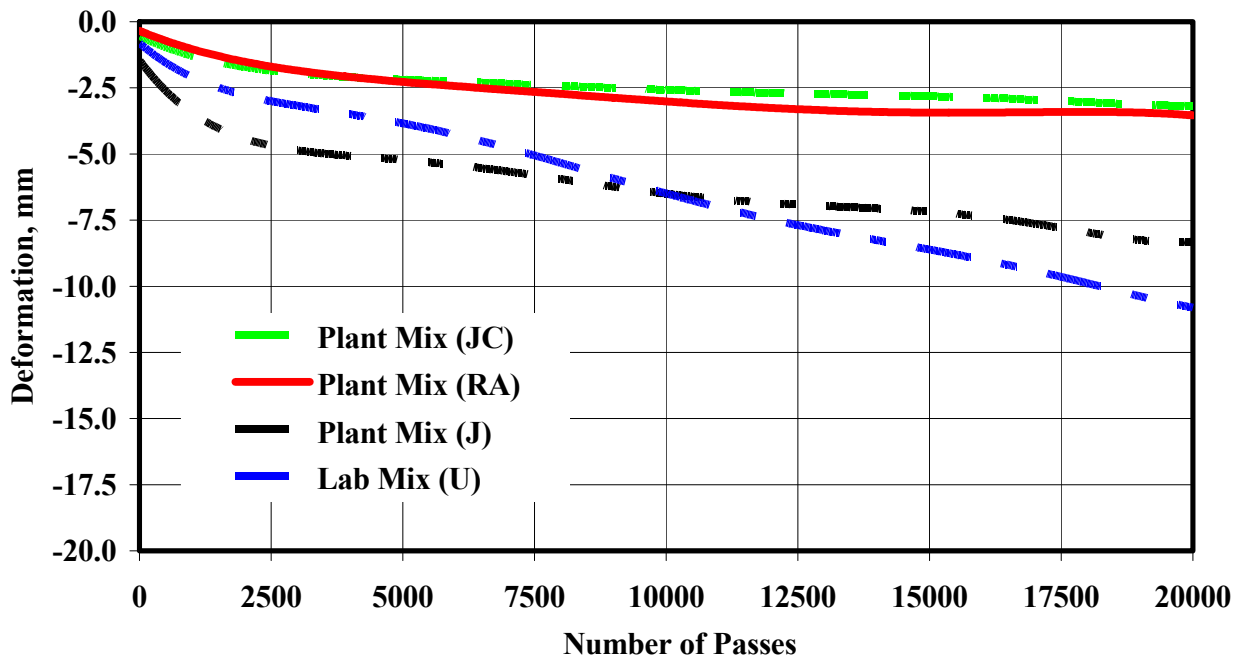
FIGURE 24   HWTD Test Results (Maximum Deformation)
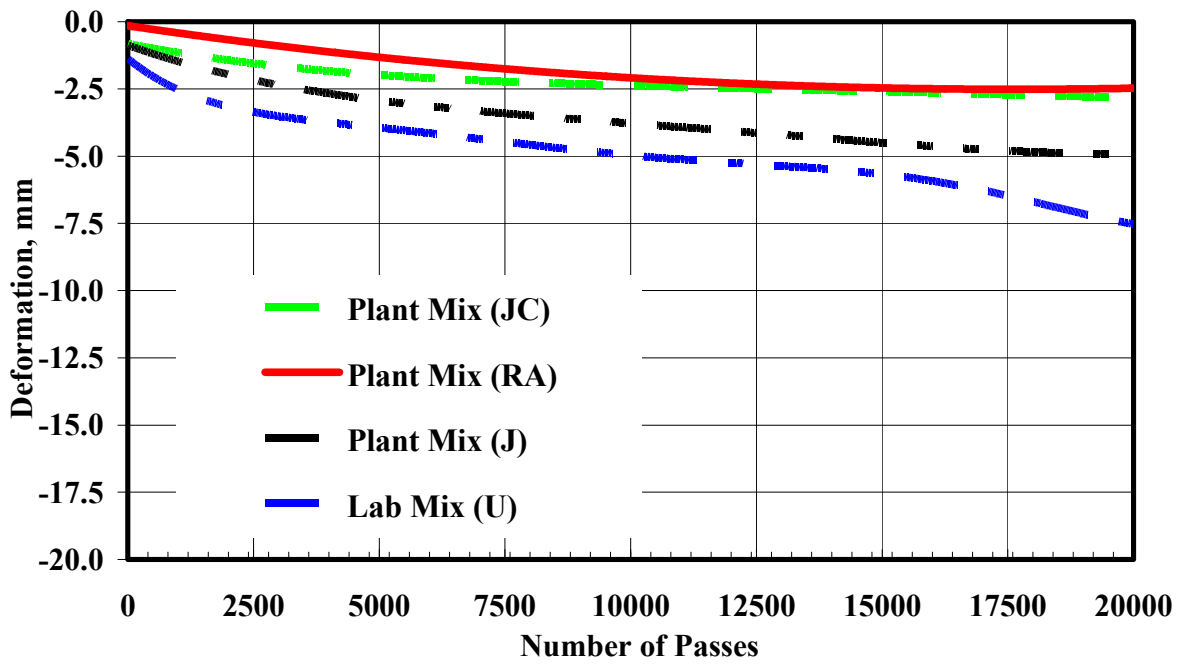
FIGURE 25   HWTD Test Results (Center of the Slab)
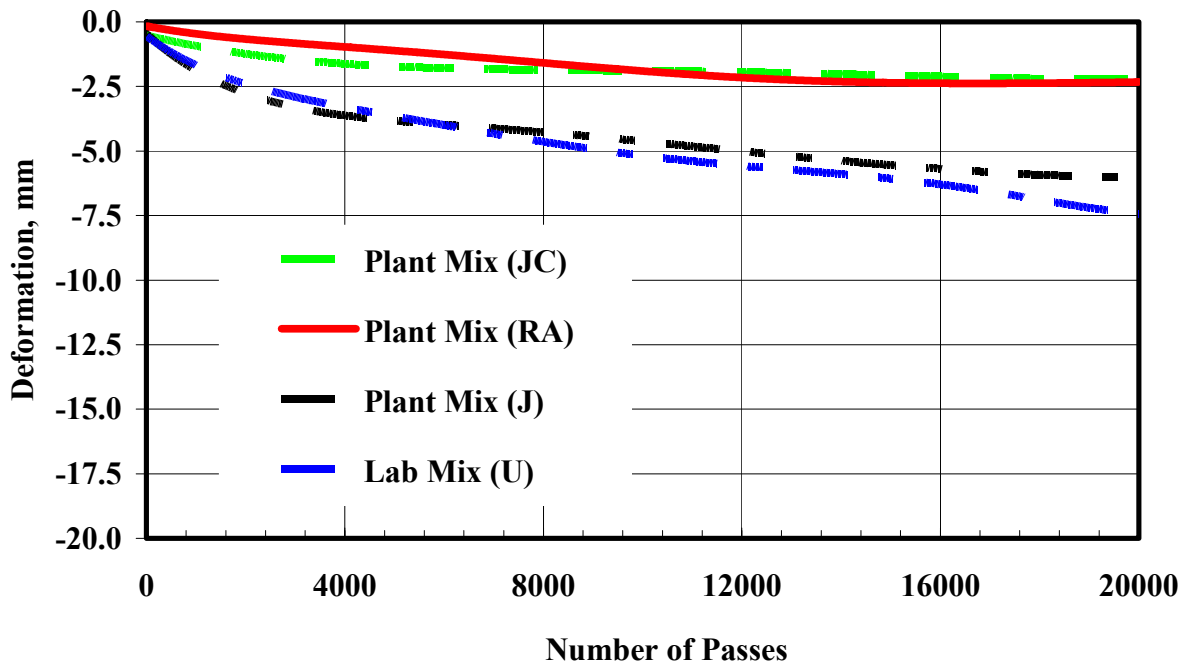
FIGURE 26   HWTD Test Results (Center of Specimen)

Although the test results presented in Figures 24 through 26 indicated that all of four mixes met the TxDOT acceptance criterion, the TxDOT experience has been that the CRM-HMAC mixes do not meet the HWTD requirements. This difference can be attributed to the modified specimen preparation process that was proposed by Swami et al. (2005). They indicated that the CRM-HMAC mixes lose temperature faster than conventional mixes, and that the specimens expand after compaction. They proposed that the specimens be compacted by heating the loose mix to 400°F, and that after compaction a stress of 600 kPa (85 psi) be maintained on the compacted specimen for 45 minutes before removal from the SGC mold. The current TxDOT specimen preparation practice consists of placing the loose mix in the mold at 325°F and letting it compact to the desired height regardless of the number of gyrations. If the specimen is compacted at higher than necessary number of gyrations, it is quite possible that the specimen may be internally damaged and may not meet the HWTD requirements. A modified specimen preparation procedure is included in Appendix B.

3.2.2   Static Creep Test Results

Three replicates of each mix were prepared by the modified procedure mentioned in the previous section, except for the Plant Mix (JC) where only one specimen was prepared and tested. The specimens were prepared as per Tex-231-F except that the specimens were compacted at 400°F. The averages of the deformations of the three specimens with time for the four mixes are included in Figure 27. A maximum deformation of more than 3 mils was observed for the Plant Mix (JC) while a minimum deformation of less than 1.25 mils was observed for the Lab Mix (U). The Plant Mix (RA) and Plant Mix (J) exhibited similar levels of deformations (around 2 mils).

Typically, the static creep test results are presented in terms of total strain, creep stiffness, and permanent strain. To obtain these parameters, the observed deformations are converted into strain as summarized in Table 3. The maximum total strains of 3.2 mils/in. were observed for the Plant Mix (JC) while minimum strain levels of 1.7 mils/in. were observed for the Lab Mix (U). Although the specimens were prepared using similar aggregate types, the Plant Mix (JC) had lower asphalt content in comparison to the Lab mix (U). The Plant Mix (RA) and (J) exhibited less total strains as compared to the Plant Mix (JC) and more than the Lab Mix (U).

The test results can also be interpreted in terms of the permanent strain. The results presented in the Table 3 suggest that the Plant Mix (RA) exhibited the lowest permanent strains of 0.90 mils/in. while the Plant Mix (J) exhibited the highest levels of permanent strains of 1.31 mils/in.

In terms of creep stiffness, the Plant Mix (RA) exhibited the highest stiffness of 5,848 psi while the Plant Mix (JC) exhibited the lowest levels of stiffness of 3,195 psi.

The coefficients of variation (COVs) varied between 6% and 46% depending on the parameters evaluated indicating that the repeatability of the test is poor and the test results may not be very reliable. It seems that more than 3 specimens need to be tested to obtain statistically reliable results. A statistical analysis performed to recommend the numbers of specimens necessary for each test is included at the end of this chapter.
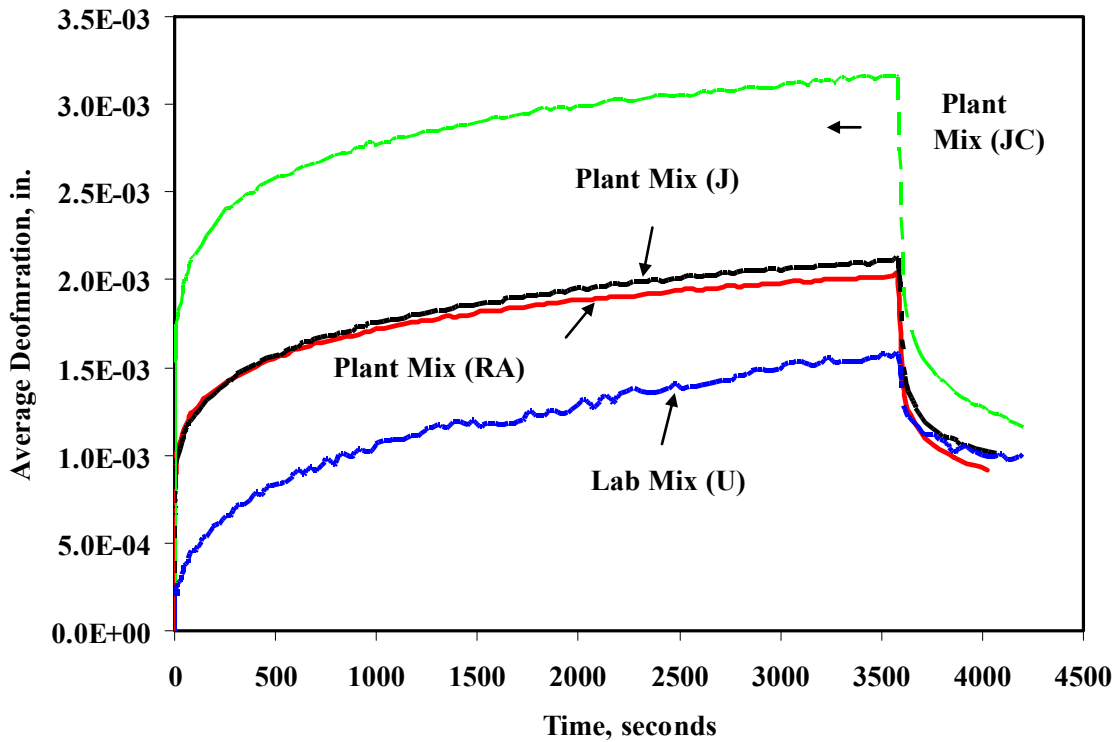
FIGURE 27 **Deformation versus Time Relationship Observed with Static Creep Testing**

TABLE 3. **Static Creep Test Results for Four Mixes**

Sample ID		Total Strain (mils/in.)	Creep Stiffness (psi)	Permanent Strain (mils/in.)
Plant Mix (RA)	Average	2.0	5,848	0.90
	S.D.	0.6	1,925	0.41
	COV (%)	31.5	32.9	45.8
Plant Mix (J)	Average	2.7	4,361	1.31
	S.D.	0.8	1,539	0.39
	COV (%)	29.0	35.3	29.6
Plant Mix (JC)	Average	3.2	3,195	1.20
	S.D.	N/A	N/A	N/A
	COV (%)	N/A	N/A	N/A
Lab Mix (U)	Average	1.7	5,602	1.21
	S.D.	0.1	352	0.31
	COV (%)	7.5	6.3	25.8
TxDOT Acceptance Criterion		≤ 2.0	≥ 4,000	≤ 0.6

As per TxDOT criterion of 2 mils/in. or less total strains, only the Plant Mix (RA) and Lab Mix (U) met the specifications. In terms of the creep stiffness, all mixes except the Plant Mix (J) met the criterion of more than 4,000 psi creep stiffness. In terms of the permanent strain, none of the mixes met the criterion of 0.6 mils/in. Since none of the mixes meet all of the TxDOT requirements, the mixes must be rejected. If the criterion for permanent strain is removed, the Plant Mix (RA) and Lab Mix (U) should perform better in comparison to the other two mixes.

3.2.3 *Indirect Tensile Strength Test Results*

The Indirect Tensile Strength (IDT) tests were performed according to Tex-26-F "Indirect Tensile Strength Test." The main difference was that the specimens were prepared using the proposed modified Tex-232-F procedure as discussed in the previous section. Three replicates of each mix were prepared except that for the Plant Mix (JC) and Lab Mix (U) only two specimens were prepared and tested. The IDT tests were performed at a temperature of 14°F rather than 77°F to assess the cracking potential of the CRM-HMAC mixes. To ensure that the specimens achieved the desired test temperatures, they were placed in a temperature-controlled chamber maintained at 14°F overnight prior to start of the test. Typical results of the load versus deformation are shown in Figure 28. The Plant Mix (RA) exhibited a higher cracking resistance (higher peak load) in comparison to the Plant Mix (J); however, the Plant Mix (J) was more ductile (more deformation before reaching peak loads) in comparison to the Plant Mix (RA). The Plant Mix (JC) and Lab Mix (U) exhibited similar levels of ductility while Lab Mix (U) exhibited higher cracking resistance in comparison to Plant Mix (JC) which is expected due to higher asphalt content.

The data reported in Figure 28 can be evaluated in three ways. In the first method, the average peak loads, which are termed as peak strengths or IDT strengths, were determined and summarized in Table 4. The four mixes yield reasonably similar average IDT strengths. The COVs varied between 3% and 35% suggesting that the test is not very repeatable, and indicating that more than three specimens need to be tested.

In the second method, the fracture energy until failure (area under the load-vertical deformation curve until maximum load) rather than maximum load is used as a parameter (as shown in Figure 28 for Plant Mix (J) to estimate the fracture energy until failure [Witczak et al., 2002]). The results of the analysis are shown in Table 5. Less fracture energy was required to fracture the Plant Mix (RA) in comparison to the Plant mix (J). This trend is contrary to the trend observed from the IDT strength tests. The explanation for this discrepancy can be found in Figure 28. The Plant Mix (RA) failed at higher loads but at very low levels of deformation (less than 0.03 in.) while the Plant Mix (J) exhibited load to failure that was lower but after deforming more than 0.06 in. Thus, the tests results suggest that the Plant Mix (J) would stretch more before cracking but can crack at lower loads in comparison to the Plant Mix (RA). Since the fracture calculations indicated different trends than observed with other tests, it may not be an appropriate approach for the CRM-HMAC mixes.

In the third method, the total fracture energy is estimating by using the whole area under the curve rather than till the peak loads. The results of the analysis are summarized in Table 5 as well. The results suggest that Lab Mix (U) required maximum energy to fracture followed by

TABLE 4.   IDT Test Results

Sample	Average Vertical Load, lbs	Indirect Tensile Strength		
		Average, psi	SD, psi	COV,%
Plant Mix (RA)	5442	433	27.2	6.3
Plant Mix (J)	5096	406	68.4	16.9
Plant Mix (JC)	4984	397	137.8	34.7
Lab Mix (U)	5268	419	15.9	3.8
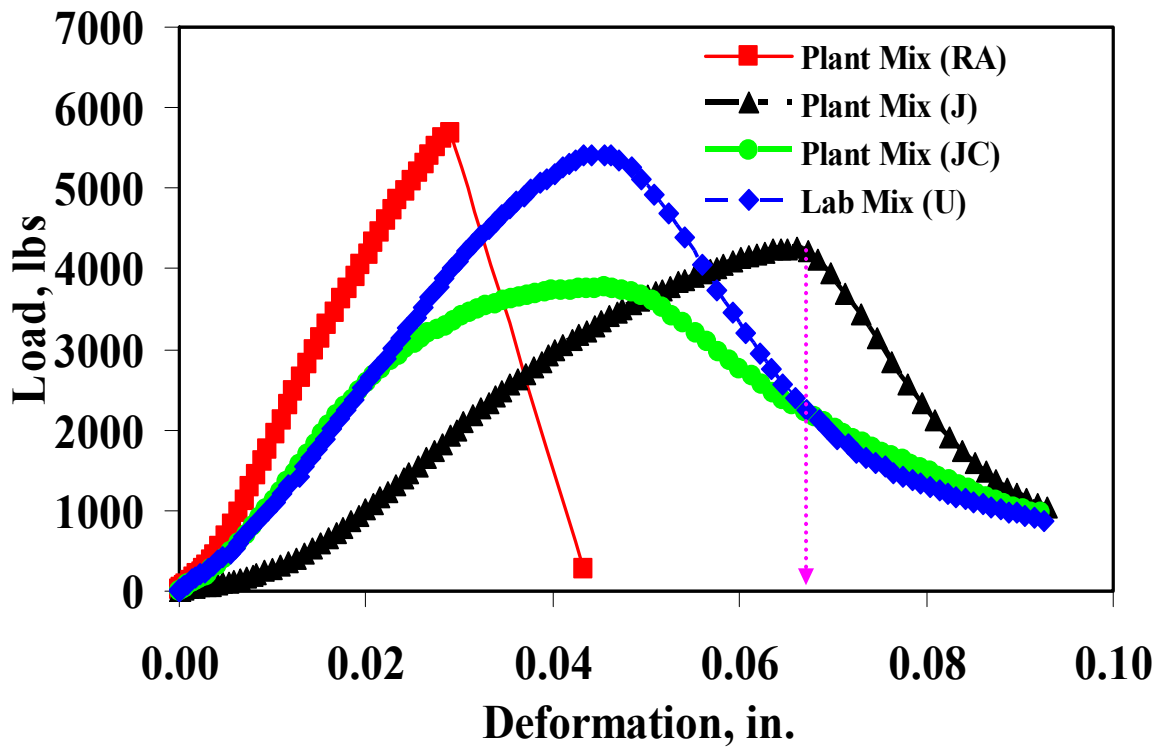
FIGURE 28   Indirect Tensile Strength Test Results

TABLE 5.   Average Fracture Energy

Material Type	Fracture Energy					
	Energy to Failure			Total Energy		
	Average, lbs-in.	SD, lbs-in.	COV, %	Average, lbs-in.	SD, lbs-in.	COV, %
Plant Mix (RA)	78	10.3	13.2	123	3.5	2.8
Plant Mix (J)	103	37.1	36.1	161	45.0	27.9
Plant Mix (JC)	124	1.1	0.9	173	59.0	34.0
Lab Mix (U)	100	15.4	15.4	242	15.0	6.1

Plant Mix (JC). This trend is distinctively different than any other test results; thus, it may not be an appropriate approach for the CRM-HMAC mixes.

3.2.4 Dynamic Modulus Test Results

The dynamic modulus tests were performed on triplicate specimens for three mixes. For the Plant Mix (JC), the tests were performed only on one specimen because of the shortage of the material. Each specimen was tested in an increasing order of temperature, i.e., 14, 40, 73, 100 and 130°F (-10, 4, 23, 38 and 54°C). For each temperature level, the specimens were tested in a decreasing order of frequency, i.e., 10, 5, 2, and 1 Hz. This temperature-frequency sequence was carried out to minimize damage to the specimen.

A typical result for the Plant Mix (RA) is shown in Figure 29. The estimated dynamic moduli decreased with the increase in the temperature and the decrease in the loading frequency (longer loading time) as expected. The data gathered at each temperature is shifted horizontally to develop a master curve at 73°F, as shown in Figure 30. This means that the data measured at a temperature higher than 73°F is shifted to the left while the data measured at a temperature lower than 73°F is shifted to the right, as shown in Figure 30. The main advantage of developing the master curve is that the data obtained from different mixes can be easily compared.

For comparison purposes, the estimated dynamic moduli at each temperature and each frequency were averaged before developing the master curve at 73°F. The shift factor versus temperature for each mix is shown in Figures 31. The coefficients of determination for all mixes are more than 0.98 indicating that the log of the shift factors are linearly dependent on temperature (i.e., all four materials are linearly viscoelastic materials within the tested range). The Lab Mix (U) is more temperature-susceptible as compared to the other mixes because the slope of the shift factor versus temperature line is more than other mixes.

The generated master curves for all of mixes are shown in Figure 32. The Plant Mix (RA) exhibited the highest stiffness in comparison to the other mixes. Also, the Plant Mix (J) exhibited similar stiffness to the Plant Mix (RA) at higher frequencies, but the stiffness decreased at lower frequencies for that mix. The Plant Mix (JC) and Lab Mix (U) exhibited similar trends.

Witczak et al. (2002) have shown that the ratio of the dynamic modulus and the sine of the phase angle, $|E^*|/\sin\Phi$, is a good indicator of rutting susceptibility. The greater this parameter is, the less susceptible the asphalt material will be to rutting. The $|E^*|/\sin\Phi$ values determined at a test temperature of 130°F and a loading frequency of 5 Hz are shown in Table 6. As per Witczak criterion, the Plant Mix (J) is the most susceptible to rutting as compared to other mixes.

The standard deviations and COVs at each temperature and frequency are shown in Table 7. In general, the COV increased with the increase in temperature, and with the decrease in frequency. The COVs varied between 7% and 33% indicating that the test method is not reliable, and perhaps more than three specimens need to be tested to improve the reliability of the tests.
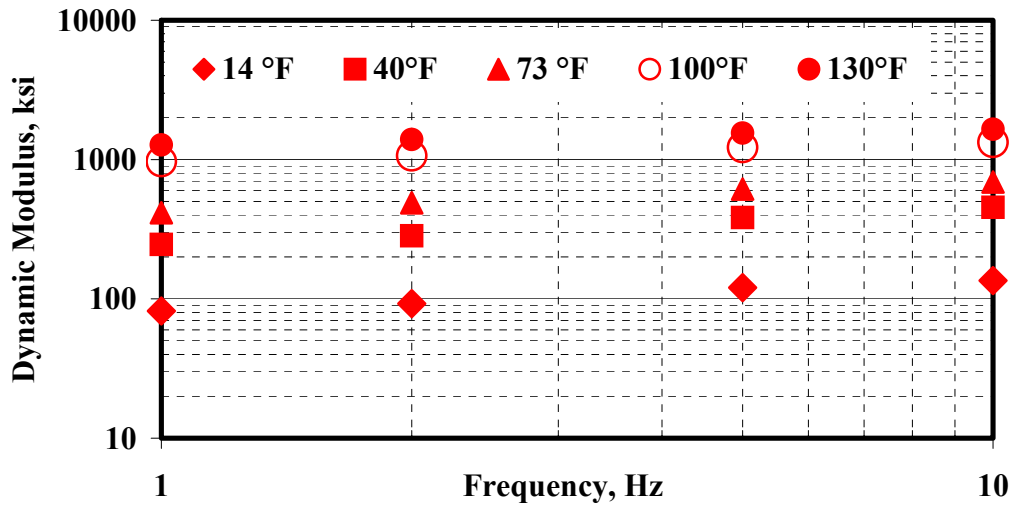
FIGURE 29   Dynamic Modulus versus Frequency Relationship for Plant Mix (RA)
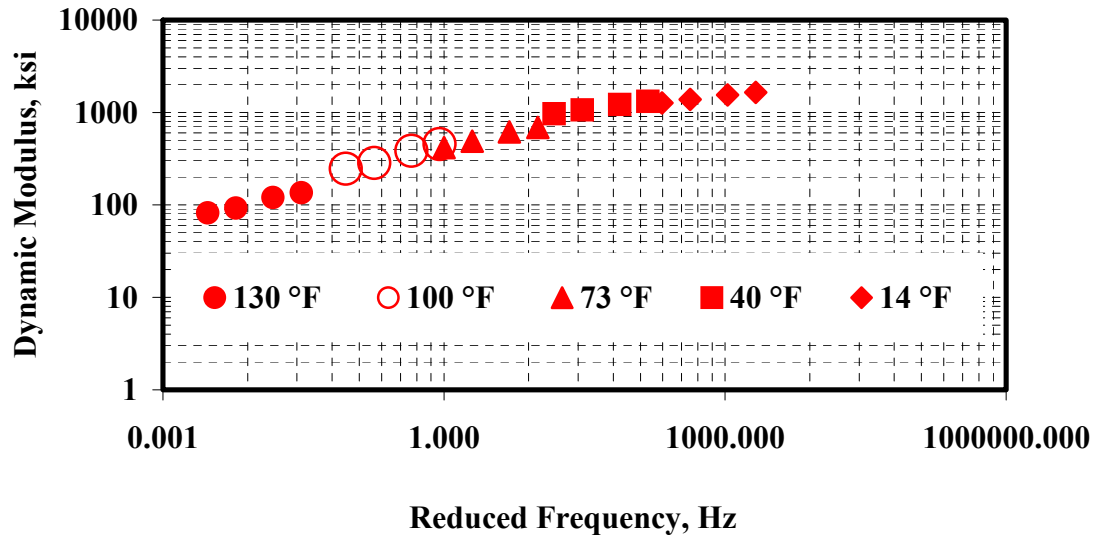
FIGURE 30   Master Curve at 73 °F for Plant Mix (RA)
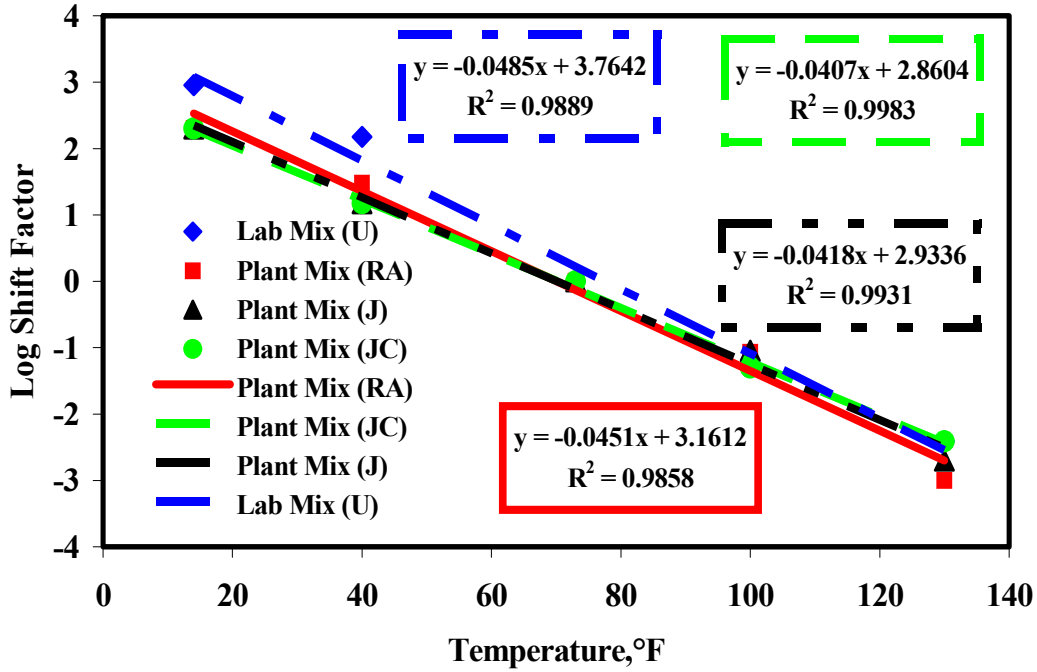
FIGURE 31   Plot of Shift factor versus Temperature

The equations shown on the plot are:

$$y = -0.0485x + 3.7642 \qquad R^2 = 0.9889$$

$$y = -0.0407x + 2.8604 \qquad R^2 = 0.9983$$

$$y = -0.0418x + 2.9336 \qquad R^2 = 0.9931$$

$$y = -0.0451x + 3.1612 \qquad R^2 = 0.9858$$

$$Log(E^*) = \delta + \frac{\alpha}{1 + e^{[\beta + \gamma \log(\frac{1}{Hz})]}}$$
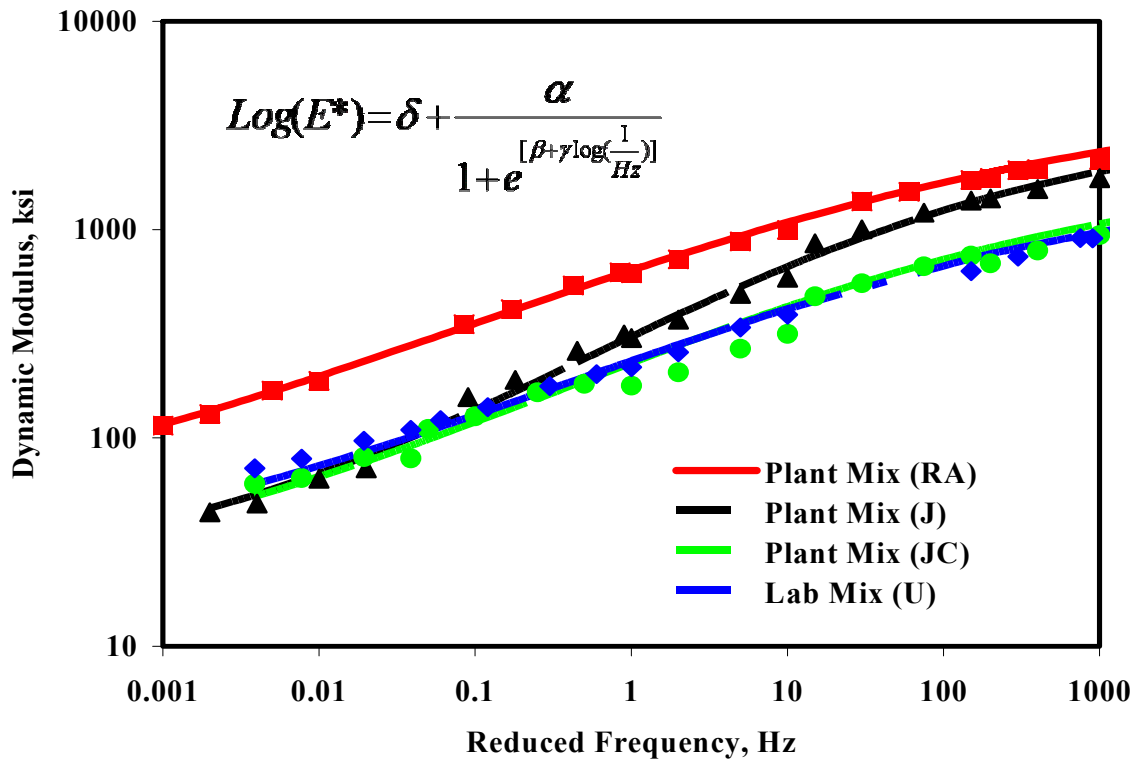
FIGURE 32   Dynamic Modulus Test Results

41

TABLE 6.   E*/sinΦ Magnitude at 130 °F and 5 Hz

Material Type	E*/sinΦ, ksi
Plant Mix (RA)	285
Plant Mix (J)	212
Plant Mix (JC)	245
Lab Mix (U)	275

TABLE 7.   Average Dynamic Modulus Values, Standard Deviation and Coefficient of Variation of Tested Mixes

Material	Temp.	130				100				73			
	Freq. (Hz)	10	5	2	1	10	5	2	1	10	5	2	1
Plant Mix (RA)	Avg (ksi).	188	169	131	114	622	539	415	352	996	878	719	617
	S.D. (ksi)	55.5	44.5	35.4	29.8	152.5	140.1	119.9	98	294.3	252.7	224.1	198
	Cov. (%).	29.5	26.3	27.0	26.1	24.5	26.0	28.9	27.8	29.5	28.8	31.2	32.1
Plant Mix (J)	Avg (ksi).	72	64	48.4	43.9	313.8	262.1	189.6	156.9	587.2	491.2	369.4	301.2
	S.D. (ksi)	24.2	20.9	16.6	16	88.7	81.7	69.4	58.1	80.4	84.2	77.1	73
	Cov. (%)	33.6	32.7	34.3	36.4	28.3	31.2	36.6	37.0	13.7	17.1	20.9	24.2
Lab Mix (U)	Avg (ksi).	109	97	79.4	71.5	202.1	176.6	140.3	121.4	390.2	338.4	257.8	218.1
	S.D. (ksi)	26.1	23.4	19.7	18.1	43.4	33.8	22.5	21.9	80.5	67.8	52.9	43.7
	Cov. (%)	23.9	24.1	24.8	25.3	21.5	19.1	16.0	18.0	20.6	20.0	20.5	20.0
Plant Mix (JC)	Avg (ksi).	80	81	64.2	60.2	181.5	165.6	126.9	110.4	315.5	268.1	206.6	178.2
	S.D. (ksi)												
	Cov. (%)												

Material	Temp.	40				14			
	Freq. (Hz)	10	5	2	1	10	5	2	1
Plant Mix (RA)	Avg (ksi).	1925	1729	1517	1364	2351	2156	1951	1771
	S.D. (ksi)	641.4	542.9	483	419.4	754.9	677.2	629.4	589.3
	Cov. (%)	33.3	31.4	31.8	30.7	32.1	31.4	32.3	33.3
Plant Mix (J)	Avg (ksi).	1376.8	1206	1001	860.6	1949.5	1767.6	1565.4	1412.6
	S.D. (ksi)	90.7	70	44.5	58.5	245	163.8	137.8	106
	Cov. (%)	6.6	5.8	4.4	6.8	12.6	9.3	8.8	7.5
Lab Mix (U)	Avg (ksi).	1061.8	909.7	741.7	631.9	1488	1285.4	1053.7	907.7
	S.D. (ksi)	182.8	129.9	95.4	86.6	104.7	105.6	77.6	64.7
	Cov. (%)	17.2	14.3	12.9	13.7	7.0	8.2	7.4	7.1
Plant Mix (JC)	Avg (ksi).	749.6	666.5	552.9	478.4	1106.0	941.5	792.7	689.6
	S.D. (ksi)								
	Cov. (%)								

3.2.5   Flow Number Test Results

Three replicates of each mix were prepared using the procedure mentioned in previous section. The flow number tests were performed at a test temperature of 140°F (54°C) and a stress level of 30 psi (210 kPa). The accumulation of strain with the number of repeated loads is plotted to identify when the flow occurred. For comparison purposes, the cumulative strain obtained from each mix is shown in Figure 33. The Plant Mixes (J) and (JC) are rut susceptible as they flowed

before the completion of 10,000 cycles. The Plant Mix (RA) and Lab Mix (U) are not rut susceptible because they did not flow till the end of 10,000 cycles.
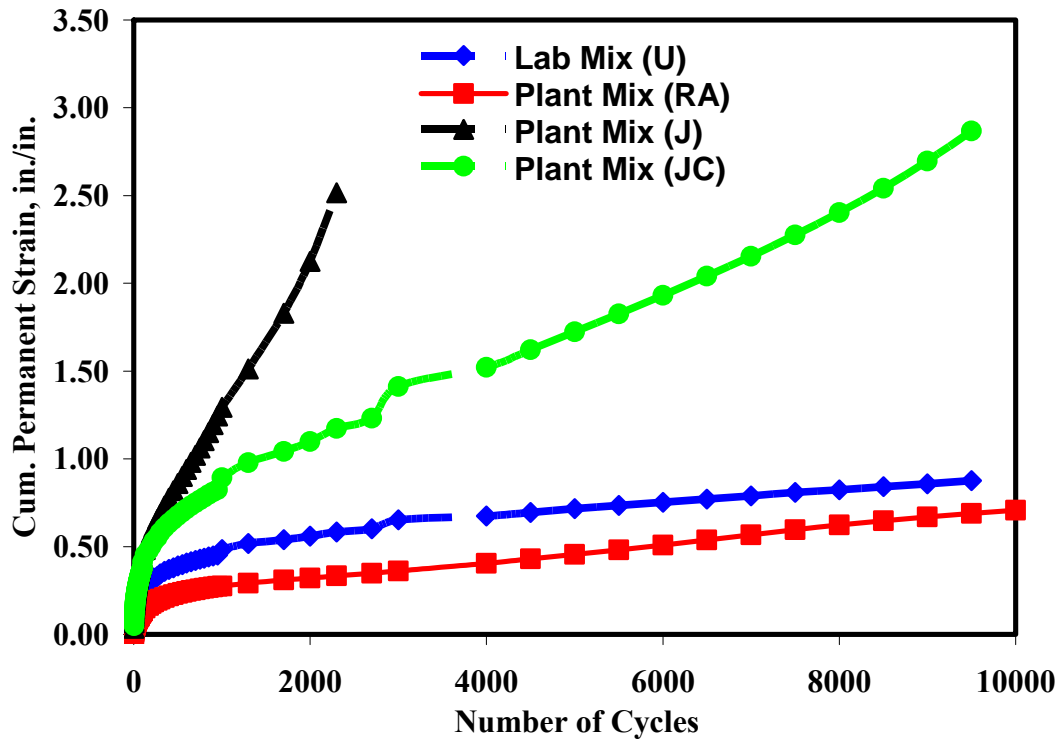
FIGURE 33   Flow Number Plots

The flow number results are shown in Tables 8. The Plant Mix (J) failed around 2,200 cycles of load while the Plant Mix (JC) failed around 6,200 cycles. The Plant Mix (RA) and Lab Mix (U) exhibited no sign of failure indicating that these mixes are better in comparison to the other mixes.

To compare the repeatability of the test, the average cumulative strains at the end of 10,000 cycles or at the time of failure are reported in Table 9. The Plant Mix (J) deformed the most and the Plant Mix (RA) the least. The COV for the mixes varied between 2% and 44% indicating a lack of repeatability with three specimens. Therefore, more than three specimens need to be tested to improve the reliability of the test.

3.2.6   Flow Time Test Results

Three replicates of each mix were prepared by the procedure mentioned in previous section. Testing was done at temperature 140°F (54ºC). A static load of 25 lb prior to the starting of the test and a constant load of 375 lb (to produce 30 psi stress) for three hours were applied to each specimen. The applied load and the resulting displacement of the specimen were continuously recorded. The axial strain with time for each mix is plotted in Figure 34 to assess the rutting potential. The data presented in Figure 34 is the average of the results from the three specimens. The Plant Mix (J) flowed in less than 3,500 seconds while Plant Mix (JC) flowed at the end of

TABLE 8.   Flow Number Test Results

Material Type	Average Flow Number	S.D. (COV.)	COV. (%)
Plant Mix (RA)	No Flow till 10,000 cycles	N/A	N/A
Plant Mix (J)	2,200	264.6	12.02
Plant Mix (JC)	6,200	282.8	4.6
Lab Mix (U)	No Flow till 10,000 cycles	N/A	N/A

TABLE 9.   Permanent Strain at the end of Flow Number Tests

Material Type	Average Permanent Strain	S.D.	COV. (%)
Plant Mix (RA)	0.6721	0.05	7.44
Plant Mix (J)	3.7582	1.65	43.9
Plant Mix (JC)	3.0786	0.29	9.42
Lab Mix (U)	0.8607	0.02	2.32
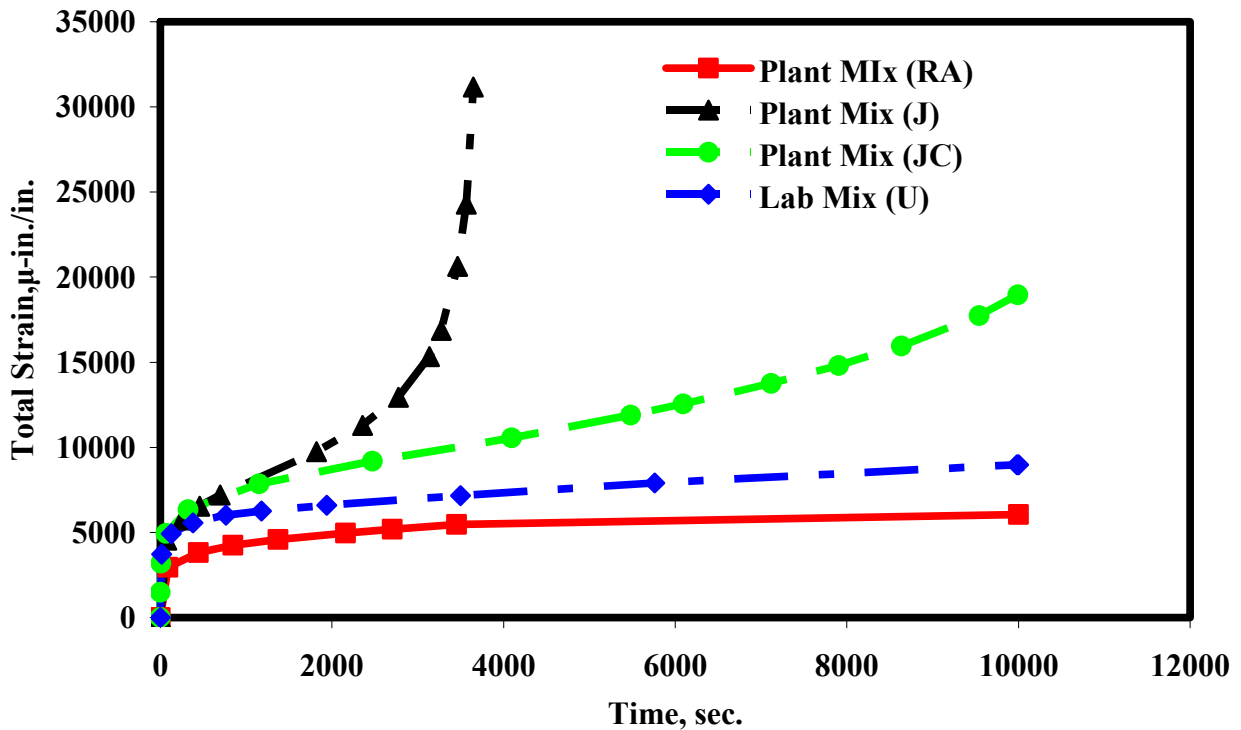
FIGURE 34   Flow Time Plot

10,000 seconds. However, the Plant Mix (RA) and Lab Mix (U) did not fail till the end of the 10,000 seconds of loading indicating that they may not be rut susceptible.

The data presented in Table 10 suggests that this test is reasonably repeatable with COVs of less than 9%. Since the Plant Mix (RA) and Lab Mix (U) did not fail, it is difficult to estimate the repeatability for those mixes.

TABLE 10.   Time at which Mixes Flowed under Flow Time Load Applications

Material Type	Flow Time	S.D., Sec.	COV, %
Plant Mix (RA)	No Flow till 10,000 sec.	N/A	N/A
Plant Mix (J)	3330	286.7	8.7
Plant Mix (JC)	9950	70.7	0.7
Lab Mix (U)	No Flow till 10,000 sec.	N/A	N/A

3.2.7   *Flexural Beam Fatigue Test Results*

The flexural fatigue beam tests were only performed on Plant Mix (J) and Plant Mix (RA). Tabular summaries of the fatigue test results and regression coefficients are presented in Tables 11 through 14. Fatigue relationships (flexural strain versus the number of loading cycles) for each mixture are shown in Figures 35 and 36. Figures 37 through 40 present comparisons of fatigue relationships for both mixtures at three temperatures, and with three Arizona gap graded asphalt rubber mixtures (ARAC).

Table 14 summarizes the K_1-K_3 coefficients of the generalized fatigue model for the Plant Mix (J) and (RA) mixtures as well as three other Arizona gap-graded asphalt rubber mixes. The relationships obtained in Tables 13 and 14 are very good to excellent measures of the models' accuracy as indicated by the coefficient of determination (R^2). Comparing fatigue curves for different mixes is not straightforward because of the different mixes' moduli. A look at the fatigue models coefficients may provide some guidance. Therefore, the comparisons are made in the following paragraph.

The results in Figures 35 and 36 are rational in that higher fatigue life is observed at the higher temperatures. Figures 37 through 39 show a comparison of the fatigue curves for the two Plant Mixes (RA and J) mixtures at the three test temperatures. The relationships shown in the figures suggest that Plant Mix (J) mixture has a better fatigue life than the Plant Mix (RA) mixture. This relationship is rational considering the difference in binder content of the two mixtures. Plant Mix (J) mixture had a higher binder content than the Plant Mix (RA). Figure 40 shows a comparison of the two mixtures with three Arizona gap graded asphalt rubber mixtures tested at ASU. Except for the Buffalo Range mixture (the first asphalt rubber mixture tested at ASU), all of the mixtures appears to have similar trends. Thus, both of the Plant Mixes fit in within the general fatigue relationships developed for the Arizona asphalt rubber gap-graded mixtures.

45

TABLE 11.   Control Strain Beam Fatigue Test Results for Plant Mix (J) Mix at 100, 70, and 40°F

Beam #	Temp [F]	Air Void %	Width (mm)	Ht. (mm)	Strain Level (≅e)	Initial Stiffness (10³psi)		50% of Initial Stiffness				30% of Initial Stiffness			
						50 cycles	100 cycles	Stiffness (ksi)	Cycles	Phase Angle	Cum. Energy (psi)	Stiffness (ksi)	Cycles	Phase Angle	Cum. Energy (psi)
SWI19	100	7.5	67.2	52.2	1,700	65.845	62.654	32.922	20,740	46.8	1402.030	#N/A	#N/A	#N/A	#N/A
SWI17	100	7.2	65.8	52.8	1,100	64.975	62.364	32.197	135,940	46.7	4022.770	17.839	152,880	-37.1	4394.924
SWI18	100	7.2	65.8	52.8	1,000	68.310	66.860	33.503	248,790	42.9	6560.261	18.129	285,810	-45.9	7177.955
SWI20A	100	6.6	67.1	53.0	800	63.524	62.074	31.762	1,363,710	46.1	21456.998	17.259	2,558,920	39.0	33532.125
SWI23	100	7.1	65.7	52.4	650	116.171	115.446	58.013	1,275,140	44.3	20093.546	32.052	4,053,690	24.0	53445.685
SWI24	70	7.4	64.6	52.8	1,400	396.664	353.154	197.244	1,370	32.6	248.441	117.186	4,090	32.9	628.861
SWI07	70	7.0	65.7	54.6	1,100	314.721	296.737	157.360	10,360	45.2	1261.929	#N/A	#N/A	#N/A	#N/A
SWI06	70	7.1	65.1	53.7	1,000	338.941	320.812	168.238	11,590	43.0	1245.830	101.523	35,490	38.8	3096.012
SWI05	70	6.7	65.7	52.8	900	423.785	403.481	211.893	13,400	41.2	1394.344	125.018	62,100	39.7	5077.883
SWI03	70	6.8	64.1	52.4	700	560.696	547.933	279.913	96,090	37.0	6693.256	165.772	171,960	34.0	11001.450
SWI09	70	7.3	66.4	52.8	600	372.734	358.231	186.367	222,450	39	8645.685	#N/A	#N/A	#N/A	#N/A
SWI04	70	6.7	64.8	52.5	500	627.411	613.488	313.561	212,710	38.6	8698.187	#N/A	#N/A	#N/A	#N/A
SWI11e	40	7.4	66.1	53.7	1,000	819.144	859.898	407.542	5,730	28.2	724.728	245.540	9,270	26.6	1118.057
SWI12b	40	7.4	66.9	54.0	900	783.031	800.580	391.153	7,660	29.9	797.825	234.228	12,670	30.3	1228.426
SWI14	40	7.2	66.3	53.9	700	1078.463	1028.136	536.186	19,610	25.7	1541.987	319.217	35,490	29.3	2600.145
SWI10c	40	6.7	64.8	52.5	500	1068.165	1053.227	530.674	78,550	23.8	3459.463	317.766	139,020	22.8	5524.003
SWI15b	40	6.7	67.1	52.8	400	936.186	933.140	461.784	440,310	21.8	11994.634	271.211	526,660	22.9	13660.044

TABLE 12.   Control Strain Beam Fatigue Test Results for Plant Mix (RA) Mix at 100, 70, and 40°F

Beam #	Temp [F]	Air Void %	Width (mm)	Ht. (mm)	Strain Level (0e)	Initial Stiffness (10³psi)		50% of Initial Stiffness				30% of Initial Stiffness			
						50 cycles	100 cycles	Stiffness (ksi)	Cycles	Phase Angle	Cum. Energy (psi)	Stiffness (ksi)	Cycles	Phase Angle	Cum. Energy (psi)
SII16B	100	7.4	64.9	52.1	1,900	106.019	101.813	52.792	2,140	41.0	324.583	31.472	2,740	41.1	379.695
SWII15	100	6.7	65.4	52.8	1,700	85.569	81.073	42.640	12,120	45.6	1101.958	24.656	72,630	46.7	4763.887
SWII14	100	6.9	65.6	51.9	1,100	115.881	111.530	57.868	118,850	50.7	5586.077	34.518	300,940	45.2	11658.013
SWII17	100	7.1	66.1	53.4	850	144.162	137.201	72.081	147,020	44.4	4956.490	43.220	1,090,190	39.0	27493.256
SWII13	100	7.1	65.3	53.0	600	124.438	119.507	62.074	1,333,530	44.4	19775.780	37.128	2,699,300	39.2	35073.387
SWII04	70	7.6	66.6	52.7	1,000	637.273	584.627	316.751	2,960	37.7	439.594	191.008	7,830	35.9	990.428
SWII03	70	7.3	68.7	55.7	900	446.265	427.556	222.625	13,400	40.1	1320.957	132.415	21,450	36.2	1923.423
SWII05	70	7.1	65.0	54.0	600	463.524	466.715	231.472	56,780	39.2	2771.284	136.911	135,940	38.4	5617.259
SWII06	70	7.8	67.9	52.5	500	821.175	812.038	408.557	147,020	29.5	6363.597	239.884	212,710	29.4	8696.012
SWII07	70	7.4	65.3	53.0	400	474.837	453.372	237.273	503,600	35.3	11258.158	138.071	901,290	32.5	17010.587
SWII10	40	6.9	66.2	53.1	600	1277.592	1025.381	634.083	16,210	14.0	733.140	377.375	32,090	10.5	1335.170
SWII08	40	7.0	64.2	52.9	400	1534.880	1544.162	766.352	389,300	17.3	11828.571	446.555	486,970	18.2	14280.203
SWII12	40	7.0	67.2	55.2	300	1214.793	1222.190	603.916	1,066,050	17.9	17583.756	354.315	1,233,030	21.1	19800.870

TABLE 13. Summary of Regression Coefficients for the Fatigue Relationships at 50% of Initial Stiffness

Mix Type	Va [%]	Test Temperature °F								
		100			70			40		
		K1	K2	R^2	K1	K2	R^2	K1	K2	R^2
Plant Mix (J)	7.0	2.41E-09	4.6747	0.950	6.08E-12	5.0852	0.951	8.50E-11	4.5805	0.975
Plant Mix (RA)	7.5	8.50E-11	5.0289	0.947	2.21E-12	5.1044	0.970	2.9E-16	6.1574	0.963
ADOT Buffalo Range ARAC	11.0	2.00E-07	4.035	0.940	3.00E-08	3.8990	0.940	8.00E-20	7.194	0.960
ADOT Two Guns ARAC	9.0	3.40E-14	5.9753	0.581	1.00E-14	5.7884	0.913	2.70E-14	5.4305	0.842
ADOT I-17 ARAC AR58-22	8.0	3.79E-16	6.8293	0.980	2.78E-14	5.8065	0.922	3.10E-15	5.8077	0.952

* $N_f = K_1 * (1/\varepsilon_t)^{K2}$

TABLE 14. Summary of the Regression Coefficients for Generalized Fatigue Equation

Mix Type	Va [%]	50% of Initial Stiffness, So @ N=50 Cycles			
		K_1	K_2	K_3	R_2
Plant Mix (J)	7.0	2.71E-04	6.051	2.013	0.992
Plant Mix (RA)	7.5	1.40E-01	4.377	1.498	0.849
ADOT Buffalo Range ARAC	11.0	2.50E-02	4.231	1.267	0.750
ADOT Two Guns ARAC	9.0	1.2E-08	8.177	2.602	0.798
ADOT I-17 ARAC AR58-22	8.0	9.38E-02	3.726	1.035	0.835

* $N_f = K_1 * (1/\varepsilon_t)^{K2} * (1/So)^{K3}$

Fatigue Relationship for Plant Mix (J) at Control Strain and 40,70 and 100 F at 50% of Initial Stiffness

$Nf(100) = 2.41E\text{-}09e^{-4.6747}$
$R^2 = 0.9504$

$Nf(40) = 8.50E\text{-}11e^{-4.5805}$
$R2 = 0.9746$

$Nf(70) = 6.08E\text{-}12e^{-5.0852}$
$R^2 = 0.9510$
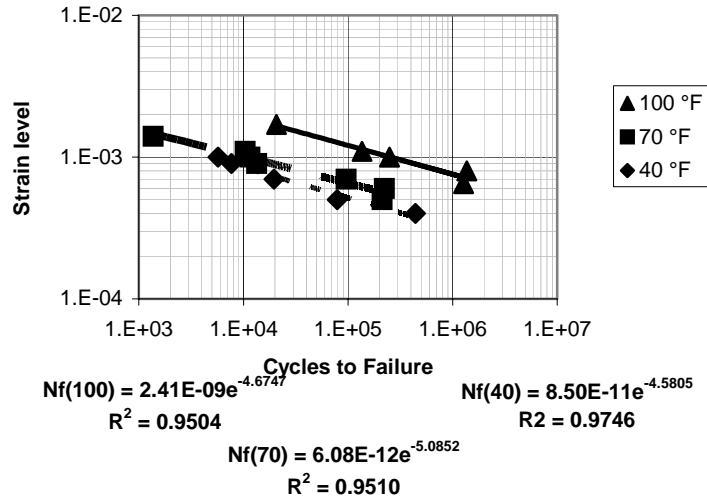
FIGURE 35   Controlled Strain Fatigue Relationships for the Plant Mix (J)

Fatigue Relationship for Plant Mix (RA) at Control Strain and 40,70 and 100oF and at 50% of Initial Stiffness

$Nf(100) = 8.496E\text{-}09e^{-5.0289}$
$R^2 = 0.9472$

$Nf(40) = 2.873E\text{-}16e^{-6.1574}$
$R2 = 0.9631$

$Nf(70) = 2.210E\text{-}12e^{-5.1044}$
$R^2 = 0.9696$
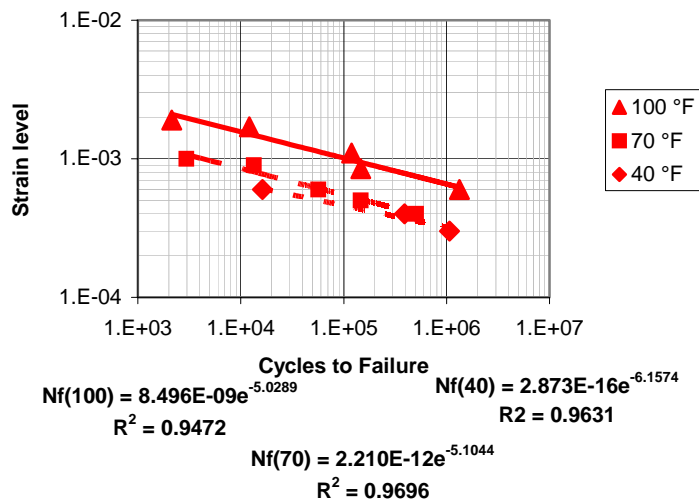
FIGURE 36   Controlled Strain Fatigue Relationships for the Plant Mix (RA)

**Comparison of the Controlled Strain Fatigue Relationships
for the two Plant Mixtures at 100°F**

Plant Mix (J)
Nf(100) = 2.41E-09e$^{-4.6747}$
R^2 = 0.9504

Plant Mix (RA)
Nf(100) = 8.496E-09e$^{-5.0289}$
R^2 = 0.9472
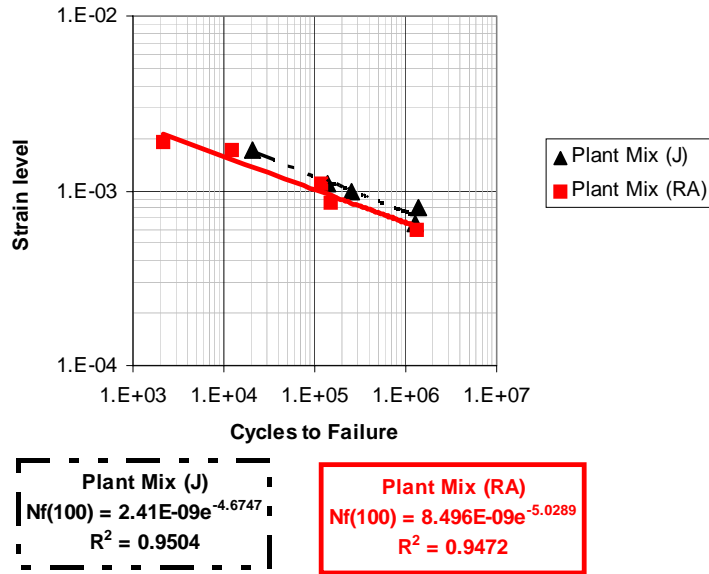
FIGURE 37   Comparison of the Fatigue Relationships at 100°F

**Comparison of the Controlled Strain Fatigue
Relationships for the two Plant Mixtures at 70°F**

Plant Mix (J)
Nf(70) = 6.08E-12e$^{-5.0852}$
R^2 = 0.9510

Plant Mix (RA)
Nf(70) = 2.210E-12e$^{-5.1044}$
R^2 = 0.9696
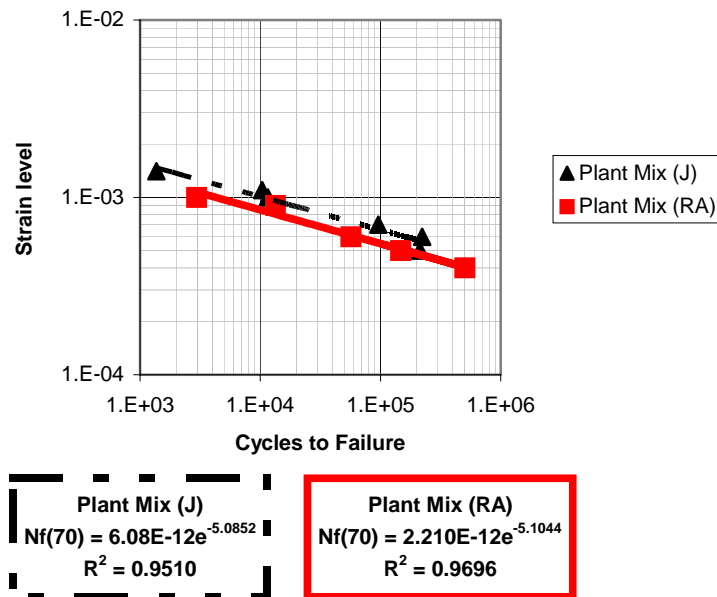
FIGURE 38   Comparison of the Fatigue Relationships at 70°F

Comparison of the Controlled Strain Fatigue Relationships for the two Plant Mixtures at 40°F

Plant Mix (J)
$Nf(40) = 8.50E-11e^{-4.5805}$
$R^2 = 0.9746$

Plant Mix (RA)
$Nf(40) = 2.873E-16e^{-6.1574}$
$R^2 = 0.9631$
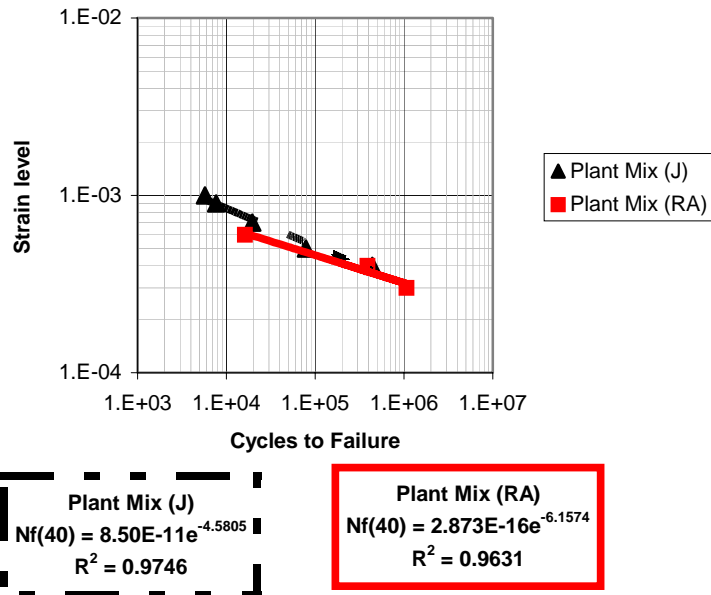
FIGURE 39   Comparison of the Fatigue Relationships at 40°F

Plant Mix (J) AV=7%
$y = 6.1E-12x^{-5.0852}$
$R^2 = 0.951$

ADOT Buffalo Range ARAC AV=11%
$y = 3E-08x^{-3.8990}$
$R^2 = 0.940$

ADOT I-17 ARAC AR58-22 AV=8%
$y = 2.8E-14x^{-5.8065}$
$R^2 = 0.922$

Plant Mix (RA) AV=7.5%
$y = 2.2E-12x^{-5.1044}$
$R^2 = 0.970$

ADOT Two Guns ARAC AV=9%
$y = 1.00E-14x^{-5.7884}$
$R^2 = 0.913$
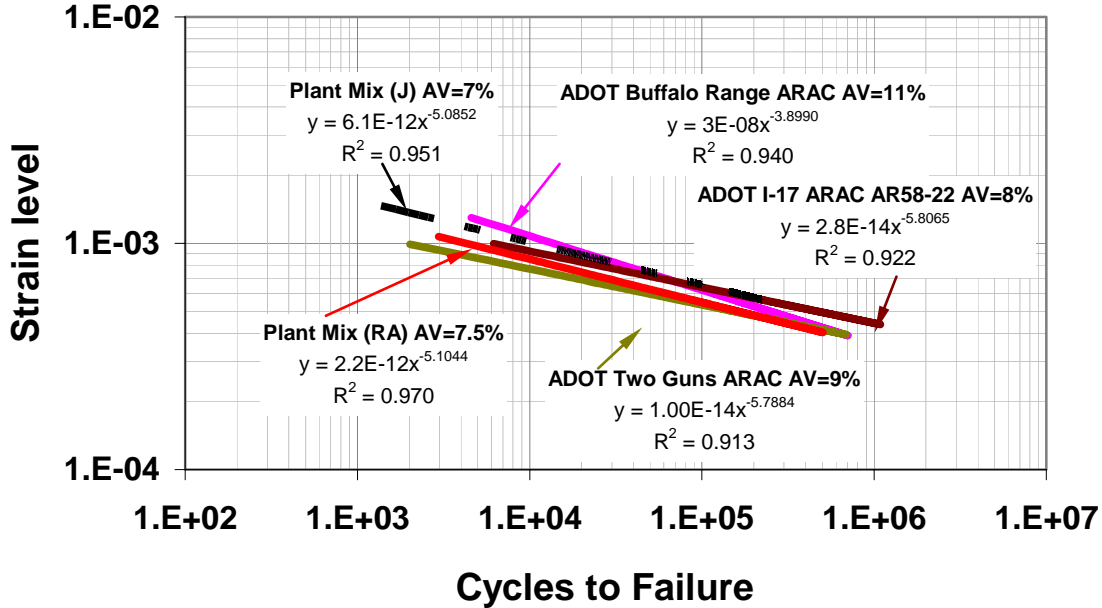
FIGURE 40   Comparison of Fatigue Relationships between Plant Mixes (J) and (RA) and Arizona Asphalt Rubber Asphalt Concrete Mixes Tested at 70°F Under Control Strain Conditions

3.2.8   Seismic Modulus Test Results

The specimens prepared for the dynamic modulus tests were also tested to determine their seismic moduli. Since seismic modulus is a non-destructive test, the seismic modulus tests were performed before dynamic modulus tests. The seismic modulus tests were performed on each specimen three times. The test results are summarized in Table 15 and Figure 41. Although tests were performed on all four mixes, the results were not recorded by mistake for two of the mixes. Therefore, the test results are presented for the only two mix types.

The tests results suggest that the seismic modulus tests are a repeatable test with coefficients of variation of less than 4 %, which is significantly lower than measured with other test methods. The measured seismic moduli of the Plant Mix (RA) are higher at all temperatures as compared to the Plant Mix (J). The seismic modulus of the Plant Mix (RA) is approximately 300 ksi higher than Plant Mix (J) regardless of the temperature. In addition, the seismic modulus decreased with the increase in temperature indicating that the CRM-HMAC modulus is temperature dependent. The observed trend is similar to the one observed with the dynamic modulus measurement tests.

TABLE 15.   Seismic Modulus Test Results

Mix Type	Test Temperature, °F	Seismic Modulus		
		Average ksi	SD ksi	COV %
Plant Mix (RA)	14	3118	57.7	1.9
	40	2936	40.6	1.4
	73	2524	55.9	2.2
	100	2264	72.4	3.2
	130	1754	56.7	3.2
Plant Mix (J)	14	2735	22.0	0.8
	40	2498	24.8	1.0
	73	2098	34.8	1.7
	100	1891	12.2	0.6
	130	1396	26.1	1.9

3.3   Comparison of Performance Test Results

Although various tests were performed and the test results were analyzed individually, it is essential that the test results be compared to performance to identify a suitable test. One way to make this comparison is by ranking the mixes for individual performance test and comparing them to the perceived field performance. One of the disadvantages of this approach is that not all of the tests characterize the same properties of mixes. For example, the static creep test evaluates the stiffness as well as rutting potential of the mix while HWTD evaluates rutting potential of the mix. Therefore, it is appropriate to compare the tests that evaluate similar

characteristics of the mix. For example, the test results obtained from the HWTD tests and permanent deformation from the static creep tests can be compared to assess the rutting potential of mixes. Thus, the comparison is performed in two different modes namely: rutting and stiffness and is discussed in the following sections
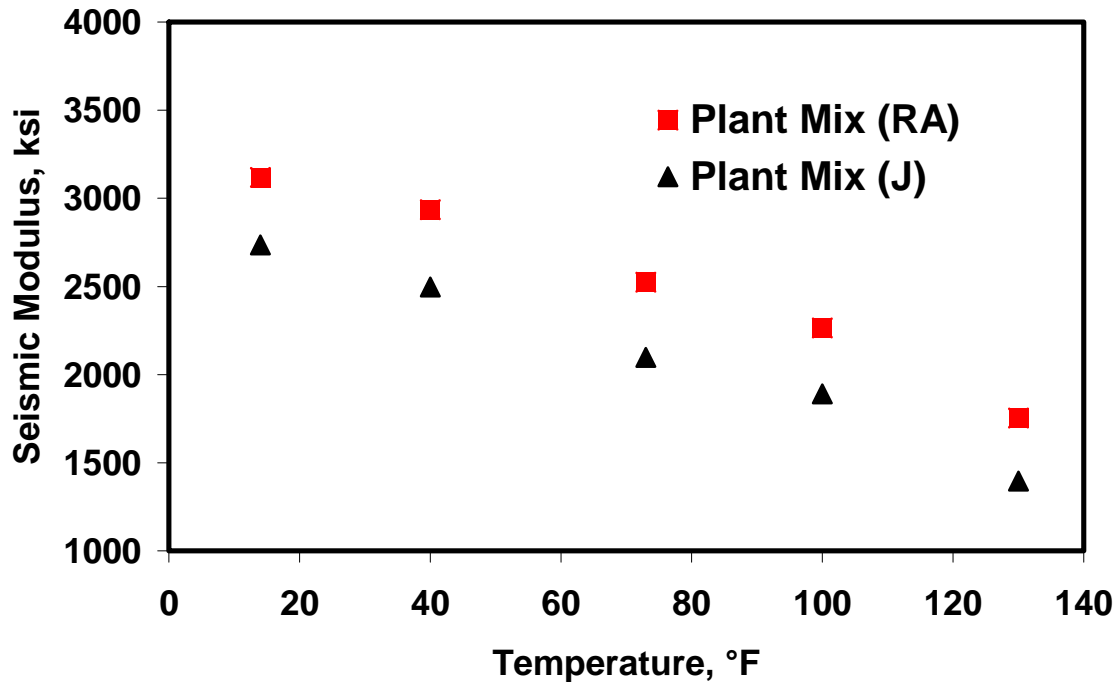
FIGURE 41   Seismic Modulus versus Temperature Relationship

3.3.1   Rutting Potential of CRM-HMAC

To compare the rankings obtained from the different performance tests, the test results from the HWTD, permanent deformation from static creep, E*/sinΦ from dynamic modulus, flow time, and flow number rankings were gathered and are summarized in Table 15. The test results clearly indicate that the Plant Mix (RA) is a superior mix in comparison to the other mixes evaluated in this study. The only exception is that the HWTD identified the Plant Mix (JC) to be the best. However, the measured deformations of 3.2 for the Plant Mix (JC) versus 3.4 for the Plant Mix (RA) are similar for all practical purposes. The test results presented in Figures 24 through 26 suggest that changing the location of permanent deformation measurement does not necessarily changes the relative ranking. Therefore, it is reasonable to suggest that Plant Mix (RA) has a better rutting resistance in comparison to the other mixes.

All performance test results suggest that the Plant Mix (J) has the highest rutting potential except for the HWTD. As per HWTD, the Lab Mix (U) has the highest rutting potential. The only explanation could be that the Plant Mix (J) and Lab Mix (U) have higher asphalt content (8.5%) than the Plant Mix (JC) and Plant Mix (RA) which have 7.5% asphalt content. The results presented in Figures 24 through 26 shows that the mixes with higher asphalt content had similar levels of permanent deformation and vice versa indicating that the HWTD may have a bias towards the percentage of asphalt content in the mixes. The conventional wisdom also suggests

53

that increasing the asphalt content may lead to a more severe rutting. However, more research is needed to draw a definite conclusion.

The test results suggest that the Lab Mix (U) has better rutting potential than Plant Mix (J) and Plant Mix (JC). The only exception is that the HWTD shows a different trend where the Plant Mix (J) and Plant Mix (JC) are considered to be better performing. Again, the only explanation could be the asphalt content.

In terms of the selection of the appropriate performance tests, it seems that most of the performance tests are providing similar ranking except the HWTD. The test results also suggest that the performance tests had similar levels of variations indicating that more specimens needed to be tested rather than three specimens used in this study.

TABLE 16.   Rutting Potential Ranking of Tested Mixes

Mix Type	Dynamic Modulus	HWTD	Static Creep	Flow Number	Flow Time
	E*/sinΦ, ksi	Maximum Permanent Deformation, in.	Permanent Deformation, mil/in.	No. of Cycles	No. of Cycles
Plant Mix (RA)	1 (285)	1 (3.4)	1 (0.90)	1 (No Flow)	1 (No Flow)
Plant Mix (J)	4 (212)	3 (8.4)	4 (1.31)	4 (2,200)	4 (3,330)
Plant Mix (JC)	3 (245)	1 (3.2)	2 (1.20)	3 (6,200)	3 (9,950)
Lab Mix (U)	2 (275)	4 (10.9)	2 (1.21)	1 (No Flow)	1 (No Flow)

3.3.2   Stiffness of CRM-HMAC

To compare the moduli obtained from different test methods, the data from the dynamic modulus, seismic modulus, indirect tensile strength, and fatigue test are ranked in Table 17. In addition to the ranking, the average value of each parameter is also included for the reference purposes. The test results clearly indicate that the Plant Mix (RA) is stiffer in comparison to the other mixes. Since the fatigue and seismic tests were performed only on two mixes; the Plant Mix (J) is considered to be number two as per these tests.

The presented IDT test results and static creep stiffness test results suggest that the Lab Mix (U) is ranked number two. However, the dynamic modulus test results suggest that it is ranked 2 at a test temperature of 130°F and ranked 3 at test temperatures of 73 and 14 °F. The change in ranking is evident in the data presented in Figure 32 which suggested that the Plant Mix (RA) is the best while other mixes are similar to each other.

Although an attempt was made to rank the mixes based on the measured material properties, the results are not changing significantly to make a statement about which mix is better. For example, the IDT strength measured varied between 433 to 397 ksi which is within the range of variability identified for the IDT test setup. Therefore, more data is needed before a definite conclusion can be drawn.

TABLE 17.   Stiffness Ranking of Tested Mixes

Mix Type	Dynamic Modulus at 10 Hz, ksi			Seismic Modulus, ksi	Creep Stiffness, ksi	IDT Strength Test, psi
	130 F	73 F	14 F	73 F		
Plant Mix (RA)	1 (188)	1 (996)	1 (2,351)	1 (2,524)	1 (5.8)	1 (433)
Plant Mix (J)	4 (72)	2 (587)	2 (1,950)	2 (2,098)	3 (4.4)	3 (406)
Plant Mix (JC)	3 (80)	4 (315)	4 (1,106)	N/T	4 (3.2)	3 (397)
Lab Mix (U)	2 (109)	3 (390)	3 (1,488)	N/T	2 (5.6)	2 (419)

Mix Type	Fatigue Stiffness, ksi					
	At 50% initial stiffness, ski			At 30% initial stiffness, ksi		
	100	70	40	100	70	40
Plant Mix (RA)	1 (58)	1 (283)	1 (668)	1 (34)	1 (68)	1 (393)
Plant Mix (J)	2 (38)	2 (202)	2 (302)	2 (21)	2 (127)	2 (278)
Plant Mix (JC)	N/T	N/T	N/T	N/T	N/T	N/T
Lab Mix (U)	N/T	N/T	N/T	N/T	N/T	N/T

3.3.3 Statistical Analysis of the Data

Although the test results suggest that HWTD provides suitable results (with modified compaction procedure), an attempt was made to identify which of the other performance tests is suitable if HWTD is not acceptable. The test results seem to indicate that almost all tests provide similar rankings of the mixes with a few exceptions. A statistical analysis, based on the Analysis of Variance (ANOVA), is typically performed to recommend a suitable test other than HWTD. However, a valid ANOVA analysis could not be performed due to the small number of specimens tested and the variability in test results. Rather than performing the ANOVA, a standard statistical analysis suggested by Walpole et al. (2002) was performed to recommend the most practical auxiliary test. According to that approach, a suitable test would be the one that provides similar levels of error with a minimum number of samples. For example, if the number of samples required to limit the error to within 10% for Test A is 20 and Test B is 10, then Test B is a more practical test. To obtain the number of samples required, the following equation can be used:

$$N \geq \left\{ \frac{Z_{\alpha/2}}{e} \right\}^2 \sigma^2 \tag{3.1}$$

where:
N = number of samples;
e = error;
σ = standard deviation of the sample;
Z = two-tailed probability statistics from the standard normal distribution;
α = confidence level.

The validity of the equation is dependent on two conditions. The first condition is that the standard deviation (SD) of the test setup is known, and the second condition is that the population average remains constant irrespective of the number of samples tested. For example, if the mean creep stiffness of 4,361 ksi is obtained by performing tests on three specimens, then the mean will be same if the number of specimens is increased to ten or higher. The SD and the mean values obtained from the tests performed were used in this analysis.

In most cases, the confidence level is set at 95% or 90% or 80% and appropriate Z values (a surrogate of probability) are determined assuming standard normal distribution. In this study, three levels of confidence of 95% (Z = 1.960), 90% (Z = 1.645) and 80% (Z = 1.282) were selected. The acceptable level of error can then be selected based on the mean values. Since the tests performed evaluated different parameters, it would be appropriate to select a percentage of the average value that is acceptable. For instance, if the measured dynamic modulus is 4,000 ksi, then ±10% acceptable error would mean that the dynamic modulus measured within 3,600 and 4,400 is acceptable. Based on these values and assumptions, Equation 3.1 was used for various tolerable error levels.

The statistical analysis of the test results for four test setups with different confidence levels are summarized in Table 18. The average and the standard deviation measured for each test setup that provided maximum variation regardless of mix type were selected. For example, the creep stiffness data obtained for the Plant Mix (J) was selected because the standard deviation was

1,539 ksi for the mix, while the Plant Mix (RA) data was selected for permanent strain because a maximum of 0.41 mil/in. was observed for the mix (Table 3).

TABLE 18.   Number of Specimens Required to Improve Reliability of Various Test Setups

Test Type		Tolerable Error (%)	Tolerable Error (e)	Number of Specimens Required			Measured	
				95%	90%	80%	Average	SD
Static Creep	Creep Stiffness, ksi	±7.5	654	21	15	9	4361	1539
		±10.0	872	12	8	5		
		±12.5	**1090**	**8**	**5**	**3**		
		±15.0	1308	5	4	2		
		±17.5	1526	4	3	2		
	Permanent Strain, mil/in.	±7.5	0.14	35	25	15	0.9	0.41
		±10.0	0.18	20	14	9		
		±12.5	**0.23**	**13**	**9**	**5**		
		±15.0	0.27	9	6	4		
		±17.5	0.32	7	5	3		
IDT	Tensile Strength, psi	±7.5	59.55	21	15	9	397	138
		±10.0	79.40	12	8	5		
		±12.5	**99.25**	**7**	**5**	**3**		
		±15.0	119.10	5	4	2		
		±17.5	138.95	4	3	2		
Dynamic Modulus Test	Dynamic Modulus, ksi	±7.5	6.59	23	16	10	43.9	16
		±10.0	8.78	13	9	5		
		±12.5	**10.98**	**8**	**6**	**3**		
		±15.0	13.17	6	4	2		
		±17.5	15.37	4	3	2		
Flow Number	Permanent Strain, in.	±7.5	0.56	33	23	14	3.7582	1.65
		±10.0	0.75	19	13	8		
		±12.5	**0.94**	**12**	**8**	**5**		
		±15.0	1.13	8	6	4		
		±17.5	1.32	6	4	3		

The creep stiffness test results suggest that an error of less than ± 7.5% can be achieved by performing tests on 21 specimens with 95% confidence and 9 specimens with 80% confidence. Since these numbers seems to be very high the error was varied up to ± 17.5% with an increment of 2.5%. The results suggest that if the tests are performed on eight specimens, then it can be stated that with 95% confidence the error will be approximately 1,090 ksi (less than ±12.5%). Since most of the HMAC tests have a variability of around 25% (or ±12.5%), the numbers of

samples required for the remainder of the test setups were determined based on this level. In terms of permanent strain, the number of specimens required for ±12.5% or less error is at least 13 specimens with a confidence level of 95% and 9 with 90% confidence. The IDT require 7 samples (with 95% confidence), while the dynamic modulus tests require 8 specimens (with 95% confidence) for an error of less than ±12.5%. The flow number test seems to require 12 specimens (with 95% confidence) to maintain a variability within ±12.5% limits.

The statistical analyses suggest that a minimum of seven specimens (with 95% confidence) or five (with 90% confidence) are required to improve the reliability of the evaluated performance tests. From the practical point of view, the only feasible test is the IDT because it can be performed quickly using Marshall Stability and Flow Meter. The required equipment is typically available within the TxDOT laboratories. The only item that needs to be added is a freezer that can be maintained at a specified temperature of 14°F. The specimens can be placed in the freezer overnight and the tests can be performed on the eight specimens quicker than any other test. Therefore, the suitable test other than HWTD is the IDT test.

CHAPTER 4   CONCLUSIONS AND RECOMMENDATIONS

To improve the durability of hot-mix asphalt concrete, crumb-rubber is typically blended within the asphalt cement. Although hot-mix asphalt concrete consisting of crumb-rubber has been successfully placed and have performed well over the years, the laboratory design and preparation of specimens are sometimes problematic. A modified design procedure was proposed in the previous report (Swami et al., 2005). The modified procedure was then used to prepare and compact specimens to identify suitable performance tests. To evaluate performance tests, four mixes were selected. Three of the mixes were obtained from the field (plant) while one of the mixes was designed at the UTEP laboratory using modified procedure.

Based on the limited evaluation of CRM-HMAC mixes, the following can be concluded:

1. The modified compaction procedure (Appendix B) does not significantly influence the performance of the mixes
2. The Plant Mix (RA) provided the best performance in comparison to the other mixes for all types of performance tests. Indicating to be a good quality mix.
3. The test results indicate that all of the test methods have a very high variability.
4. To improve reliability, the statistical analysis suggests that more than five specimens need to be prepared.
5. The HWTD can predict the performance of CRM-HMAC by utilizing the new compaction and mix handling procedure. A modified procedure for compacting specimens for performance evaluation of CRM-HMAC specimens using HWTD is included in Appendix C. It is important to keep in mind that the modified procedure is for specimen preparation in the laboratory and not for the field production or placement.
6. The test results suggest that IDT test may be the most practical test to obtain reliable results. However, more tests are needed before it can be implemented.

REFERENCES

1. Bennert, T., Maher, A., and Smith, J., "Evaluation of Crumb Rubber in Hot Mix Asphalt," Final Report, Center for Advanced Infrastructure and Transportation (CAIT), Rutgers Asphalt/Pavement Laboratory (RAPL), Rutgers University, Piscataway, NJ, July 2004.

2. Harvey, J., and Monismith, C.L., "Effect of Laboratory Asphalt Concrete specimen Preparation Variables on Fatigue and Permanent Deformation Test Results Using Strategic Highway Research Program A-003A Proposed Testing Equipment," Record 1417, Transportation Research Board, Washington, D.C., 1993.

3. Izzo, R.P., and Tahmoressi, M., "Testing Repeatability of the Hamburg Wheel-Tracking Device and Replicating Wheel-Tracking Devices among Different Laboratories," Journal of The Association of Asphalt Paving Technologists, Asphalt Paving Technology, 1999, pp. 589-612,.

4. Kaloush, K. E., Witczak, M. W., Way, G. B., Zborowski, A., Abojaradeh, M., and Sotil, A. "Performance Evaluation Of Arizona Asphalt Rubber Mixtures Using Advanced Dynamic Material Characterization Tests," Arizona Department of Transportation and FNF Construction, Inc. Final Report, Arizona State University, Tempe, Arizona, July 2002.

5. Nazarian S., Yuan D., Tandon V. and Arellano M., "Quality Management of Flexible Pavement Layers with Seismic Methods," Research Report 1735-3, The Center for Transportation Infrastructure Systems, The University of Texas, El Paso, TX, 2003.

6. Pagen, C. A. (1963), "An Analysis of the Themorheological Response of Bituminous Concrete," Master of Science Thesis, The Ohio State University, pp. 26-33.

7. Pellinen, T.K., Witczak, M.W., "Stress Dependent Master Curve Construction fro Dynamic (Complex) Modulus," Journal of Association of Asphalt Paving Technologists, Volume 71, 2002, pp. 281-309.

8. Roberts, F.L., Kandahl, P.S., Brown, E.R., Lee, D.Y., and Kennedy, T.W., *Hot Mix Asphalt Materials, Mixture Design, and Construction*, NAPA Research and Education Foundation, Lanham, MD., 1996.

9. SHRP-A-404. *Fatigue Response of Asphalt-Aggregate Mixes*. Asphalt Research Program, Institute Of Transportation Studies, University Of California, Berkeley. Strategic Highway Research Program, National Research Council, Washington, D.C., 1994.

10. Solaimanian, M., J. Harvey, M. Tahmoressi, and V. Tandon "Test Methods to Predict Moisture Sensitivity of Hot-Mix Asphalt Pavements," In Moisture Sensitivity of Asphalt Pavements (CD-ROM), TRB, National Research Council, Washington, D.C., 2004, pp. 77–110.

11. Sousa, J.B., Pais, J.C., Saim, R., Way, G.B., and Stubstad, R.N., "Development of a Mechanistic-Empirical Based Overlay Design Method for Reflective Cracking, Transportation Research Record No. 1809, Transportation Research Board, Washington, D.C., 2002

12. Swami, V., Tandon, V., and Nazarian, S. "Mix Design Procedure for Crumb Rubber Modified Hot Mix Asphalt," Report No. FHWA/TX-05/0-4821-1, Center for Transportation Infrastructure Systems, The University of Texas at El Paso, El Paso, Texas, 2005

13. Tayebali, A. A., Deacon, J. A., and Monismith, C. L., "Development and Evaluation of Surrogate Fatigue Models for SHRP. A-003A Abridged Mix Design Procedure," Journal of the Association of Asphalt Paving Technologists Vol. 64, 1995, pp. 340-366.

14. Walpole, R.E., Myers, R.H., Myers, S.L., and Ye, K., *Probability & Statistics for Engineers & Scientists*, Seventh Edition, Prentice Hall, New Jersey, 2002.

15. Witczak, M.W., Mamlouk, M., and Abojaradeh, M. *Flexural Fatigue Tests*. NCHRP 9-19, Subtask F6 Evaluation Tests. Task F Advanced Mixture Characterization. Interim Report, Arizona State University, Tempe, Arizona, July 2001.

16. Witczak, M.W., Kaloush, K., Pellinen, T., El-Basyouny, M., and Von Quintus , H., "Simple Performance Test for Superpave Mix Design", NCHRP Report 465, Transportation Research Board, Washington, D.C., 2002.

APPENDIX A: VISCOSITY VERSUS TEMPERATURE RELATIONSHIP FOR HMAC CONSISTING OF CRM BLEND

To evaluate properties of asphalt cement blended with crumb-rubber, the complex modulus and phase angle of the blend were measured at three temperatures and seventeen frequencies using dynamic shear rheometer. The measured test results have been reported in the first report of this project (Swami et al., 2005). To identify and select compaction temperatures, the complex modulus and phase angle data was used to generate viscosity versus temperature relationships based on the relationships proposed by Witczak et al. (2002) and Bennert et al. (2004). The developed relationship is presented in the Figure A1. To identify compaction temperature, the viscosity ranges suggested by SHRP were used. Based on the SHRP specifications, the required viscosity of 0.31 Pa-s is met at a minimum compaction temperature of 400 °F and should be used for compacting HMAC specimens consisting of CRM.
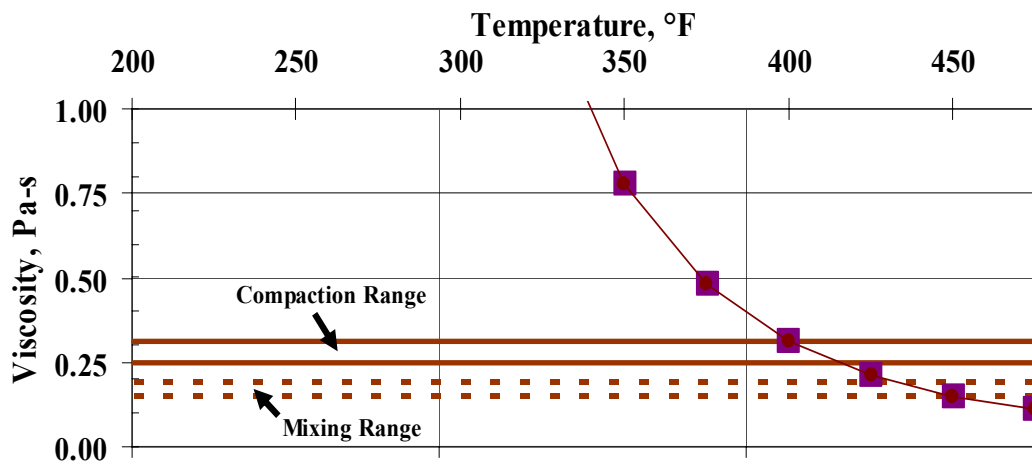
Figure A.1. Viscosity-Temperature Relationships for HMAC Consisting of CRM

APPENDIX B: METHOD OF MIXING AND COMPACTION OF HMAC CONSISTING OF CRM BLEND

Section 1: **Overview**
Use this procedure to prepare hot mix asphalt concrete specimens consisting of Crumb Rubber (CRM-HMAC) to determine the susceptibility of bituminous mixtures to moisture damage.

Units of Measurement
The values given in parentheses (if provided) are not standard and may not be exact mathematical conversions. Use each system of units separately. Combining values from the two systems may result in nonconformance with the standard.

Section 2: **Apparatus**
The following apparatus is required:

► Apparatus listed in the following test methods

- "Tex-207-F, Determining Density of Compacted Bituminous Mixtures"
- "Tex-241-F, Superpave Gyratory Compacting of Test Specimens of Bituminous Mixtures."

Mixing and Compaction of CRM-HMAC

Step	Action
1.	Obtain and weigh two separate 5.5 lb (2,500 g) samples of the CRM-HMAC mix for molding using SGC.
2.	Cure all samples in an oven preheated to 400 °F (205 °C) for 2 hours.
3.	Mold the two 2,200 lb. (1,000 g) specimens according to Test Method "Tex-241-F, Superpave Gyratory Compacting of Test Specimens of Bituminous Mixtures." • To avoid temperature loss, after pouring hot mix in the mold keep mold inside the oven for 15 minutes. • Heights must be 2.4 ± 0.1 in. (62 ± 2 mm). • Leave the samples in the molds until they are cool to touch for TGC specimens.
4.	In addition to test method Tex-241-F there are some additional steps for compacting specimen using SGC are following:- • To avoid temperature loss, after pouring hot mix in the mold keep mold inside the oven for 15 minutes. • After compacting hot mix till desired height press the emergency stop in SGC

Step	Action
	machine so that 87 psi. (600 kPa) stresses will be on specimen and leave the mold with specimen inside SGC for 45 minutes. Application of stress after compaction is to restrain the axial expansion. • After 45 minutes remove specimen from mold and tie in PVC pipe to restrain horizontal expansion before performing G_{mb}.
5.	Determine the bulk specific gravity and relative density of molded specimens according to Test Method "Tex-207-F, Determining Density of Compacted Bituminous Mixtures."
6.	Calculate the density of the molded specimens using Tex-207-F.
7.	If the molded density is less than $97 \pm 1\%$ reduce the amount of mix using weight volume relationships and vice versa.
8.	**Caution** The number of gyrations should always be lower than 75 to achieve desired density and height. The amount of mix needs to be adjusted if the number of gyrations exceeds this limit.

APPENDIX C: MODIFIED TEX-242-F, HAMBURG WHEEL-TRACKING TEST

Overview

Effective date: November 2004 (refer to 'Archived Versions' for earlier versions).

Use this test method to determine the premature failure susceptibility of bituminous mixtures due to weakness in the aggregate structure, inadequate binder stiffness, or moisture damage and other factors including inadequate adhesion between the asphalt binder and aggregate. This test method measures the rut depth and number of passes to failure.

Units of Measurement

The values given in parentheses (if provided) are not standard and may not be exact mathematical conversions. Use each system of units separately. Combining values from the two systems may result in nonconformance with the standard.

Apparatus

Use the following apparatus:

♦ Wheel-tracking Device

  • An electrically powered device capable of moving a steel wheel with a diameter of 8 in. (203.6 mm) and width of 1.85 in. (47 mm) over a test specimen.

  • The load applied by the wheel is 158 ± 5 lbs. (705 ± 22 N).

  • The wheel must reciprocate over the test specimen, with the position varying sinusoidally over time.

  • The wheel shall make approximately 50 passes across the test specimen per minute.

  • The maximum speed of the wheel must be approximately 1.1 ft./sec. (0.305 m/s) and will be reached at the midpoint of the slab.

♦ Temperature Control System

  • A water bath capable of controlling the test temperature within ± 4 °F (2 °C) over a range of 77 to 158 °F (25 to 70 °C).

  • This water bath must have a mechanical circulating system to stabilize temperature within the specimen tank.

- ♦ Rut Depth Measurement System

  - A Linear Variable Differential Transducer (LVDT) device capable of measuring the rut depth induced by the steel wheel within 0.0004 in. (0.01 mm), over a minimum range of 0.8 in. (20 mm).

  - The system shall be mounted to measure the rut depth at the midpoint of the wheel's path on the slab.

  - Rut depth measurements must be taken at least every 100 passes of the wheel.

  - This system must be capable of measuring the rut depth without stopping the wheel. This measurement must be referenced to the number of wheel passes.

  - Fully automated data acquisition and test control system (computer included).

- ♦ Wheel Pass Counter

  - A non-contacting solenoid that counts each wheel pass over the test specimen.

  - The signal from this counter must be coupled to the rut depth measurement, allowing the rut depth to be expressed as a fraction of the wheel passes.

- ♦ Specimen Mounting System

  - A stainless steel tray which can be mounted rigidly to the machine in the water bath.

  - This mounting must restrict shifting of the specimen during testing.

  - The system must suspend the specimen, allowing free circulation of the water bath on all sides.

  - The mounting system shall be designed to provide a minimum of 0.79 in. (2 cm) of free circulating water on all sides of the sample.

Materials

Use the following materials:

- ♦ Three high-density polyethylene molds shaped according to plan view in the 'Top View of Test Specimen Configuration for the Hamburg Wheel-Tracking Device' to secure circular, cylindrical test specimens. Use one mold for cutting the specimen and the other two for performing the test.

- ♦ Capping compound able to withstand 890 N (200 lb.) load without cracking.

Specimen

Laboratory Molded Specimen

Prepared according to "Tex-205-F, Laboratory Method of Mixing Bituminous Mixtures" and "Tex-241-F, Superpave Gyratory Compacting of Test Specimens of Bituminous Mixtures."

For hot mix asphalt concrete consisting of CRM Blend, the specimens be prepared according to the Method Presented in Appendix B.

Specimen diameter shall be 6 in. (150 mm) and specimen height should be 2.4 ± 0.1 in. (62 ± 2 mm).

Density of test specimens must be 93 ± 1%.

Core specimen

Specimen diameter shall be 6 ± 0.1 in. (150 ± 2 mm) or 10 ± 0.1 in. (254 ± 2 mm).

Procedure

Follow these steps to prepare and test the sample.

Sample Preparation and Testing	
Step	*Action*
1	Test requires two cylindrically molded specimens with the Superpave Gyratory Compactor according to "Tex-241-F, Superpave Gyratory Compacting of Test Specimens of Bituminous Mixtures. " ◆ Specimens must be molded to a specified density of 93 ± 1% ◆ Specimens must be molded to a specified height of 2.4 ± 0.1 in. (62 ± 2 mm). ◆ Specimen weights typically vary between 2400-2600 grams to achieve density. ◆ Specimen weights vary with different aggregate sources and with different mix types.
2	Measure the relative density of specimens according to "Tex-207-F, Determining Density of Compacted Bituminous Mixtures " and "Tex-227-F, Theoretical Maximum Specific Gravity of Bituminous Mixtures. "
3	Place a specimen in the cutting template mold and use a masonry saw to cut it along the edge of the mold. ◆ The cut across the specimen should be approximately 5/8 in. (16 mm) deep. ◆ The specimen should be cut to the dimensions shown in 'Top View of Test Specimen Configuration for the Hamburg Wheel-tracking Device' in order to fit in the molds required for performing the test.

4	♦ For specimens 6 in. (150 mm) in diameter: • Place the high-density polyethylene molds into the mounting tray and fit specimens into each one. • Secure the molds into the mounting tray. NOTE: Do not use the high-density polyethylene molds for core specimens greater than 6 in. (152 mm) in diameter. ♦ For specimens greater than 6 in. (150 mm) in diameter: • Mix capping compound. • Spray the mounting tray with a light lubricant. • Place specimen in the middle of the mounting tray. • Spread the capping compound around the core specimen until level with the surface. Allow the capping compound to dry a minimum of 24 hours.
5	Fasten the mounting trays into the empty water bath.
6	Start the software supplied with the machine and enter the required test information into the computer.
7	Test temperature shall be 122 ± 2 °F (50 ±1°C) for all hot mix asphalt specimens ♦ Fill the water bath until the water temperature is at the desired test temperature. ♦ The temperature of the water can be monitored on the computer screen. ♦ Allow the test specimen to be saturated in the water for an additional 30 minutes once the desired water temperature has been reached.
8	Start the test after the test specimens have been in the water for 30 7minutes at the desired test temperature. The testing device automatically stops the test when the device applies the number of desired passes or when the maximum allowable rut depth has been reached.
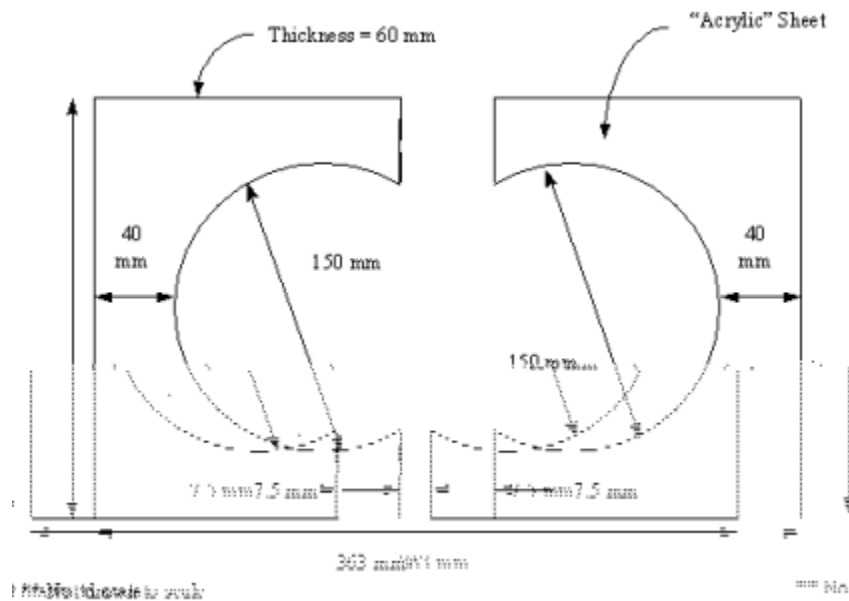
Figure 1. Top View of Test Specimen Configuration for the Hamburg Wheel-tracking Device.

Report

For each specimen, report the air void content, anti-stripping additive used, number of passes to failure and the rut depth at the end of the test.

Report Forms

- ◆ 'Hamburg Wheel-Tracking Test '